2009

# Development and commissioning of a small engine test cell

Jacob R. Brown
*West Virginia University*

# Development and Commissioning of a Small Engine Test Cell

**Jacob R. Brown**

**Thesis submitted to the**
**College of Engineering and Mineral Resources**
**at West Virginia University**
**in partial fulfillment of the requirements**
**for the degree of**

**Master of Science**
**In**
**Mechanical Engineering**

**W. Scott Wayne, Ph.D., Chair**
**Andrew Nix, Ph.D.**
**Hailin Li, Ph.D.**

**Department of Mechanical and Aerospace Engineering**

**Morgantown, WV**
**2009**

**Keywords: Dynamometer; Emissions Testing; Small Engine; Test Cell Development; TRU**

## Abstract

### Development and Commissioning of a Small Engine Test Cell

**Jacob R. Brown**

For the purposes of providing the Center for Alternative Fuels, Engines, and Emissions (CAFEE) of West Virginia University (WVU) with the ability to perform engine dynamometer and emissions testing on small engines in the range of 40 horsepower or less, a new test cell was built and commissioned within the CAFEE annex facility in the Morgantown Industrial Park in Westover, WV. The test cell was designed to be used with existing CAFEE emission testing equipment.

Test cell commissioning demonstrated the ability of the system to properly operate full steady state test cycles, as well as capture steady state continuous gaseous emissions data and gravimetric particulate matter data. During steady state tests, which followed the ISO-8178 test cycle, the dynamometer showed the capability of holding engine speed within 2% of the reference set point value, and within 1% on a mean basis. Similarly, setpoint reference torque loads between 10 and 60 ft-lbs, which were based on a full map of the test engine, the dynamometer was able to hold torque within 2% of the reference value, for each point and within 1% on a mean basis.

A series of steady state tests performed on a 4 cylinder Isuzu CP201 Transport Refrigeration Unit (TRU) diesel engine resulted in baseline engine out emissions data (g/bhp-hr) for HC, CO, CO2, NOx, and PM of 4.31, 2.71, 751.98, 7.33, and 0.591 respectively. Controlled emissions results, with an exhaust aftertreatment Diesel Particulate Filter (DPF) containing an internal catalyst layer, resulted in reduction in HC, CO, and PM of 81, 84, and 86% respectively. The reduction in PM of 86% by the DPF was within the requirements of the California Air Resources Board (CARB) Low Emission TRU (LETRU) Level 2 PM reduction requirement for Verified Diesel Emission Control Strategies (VDECS).

## Acknowledgements

I would like to extend my thanks to all of those who made the process of my graduate studies possible, memorable, and most importantly, enjoyable. First, I would like to thank Dr. Scott Wayne for giving me the opportunity to pursue my degree under his advisement. I would also like to thank my committee members, Dr. Andrew Nix, and Dr. Hailin Li for their constant and open support during this process.

A sincere thank you to Richard Atkinson, whose contributions made the electrical and data acquisition aspect of my project possible, and whose musings and teachings will never be forgotten. Thanks also, to all the CAFEE members at Westover who made this journey possible.

A special thank you to my Mother and Father for always being there for me, and providing me with the teachings, guidance, and support that have brought me so far in my life. I would not be who I am now if it were not for you both. Thank you Lucas Brown, for being the best brother and friend anyone could ask for. Thank you especially Lemma McLean, for your caring support and encouragement. To all my friends, thank you, I am so fortunate to have so many of you. Thanks Balaji Seward, and Chet-Mun Liew, not only because they are great friends, but also because I could tell they both really wanted to be mentioned in here. Finally, I would like to thank the WVU Cycling Team, Pathfinder of West Virginia, and all of the Morgantown cycling community, who provided me, an outlet for my cravings for adventure, the means to support my love for cycling, and an arena, in which, to fulfill my persistent need for enjoyment. After all, it's just a fun time.

## Table of Contents

## List of Tables

## List of Figures

# List of Abbreviations and Symbols

| | |
|---|---|
| APU | Auxiliary Power Unit |
| BC | Black Carbon |
| CAFEE | Center for Alternative Fuels, Engines, and Emissions |
| CARB | California Air Resources Board |
| CCR | California Code of Regulations |
| CFR | Code of Federal Regulations |
| CVS | Constant Volume Sampling |
| DOC | Diesel Oxidation Catalyst |
| DPF | Diesel Particulate Filter |
| DNA | Deoxyribonucleic Acid |
| EERL | Engines and Emissions Research Laboratory |
| EPA | Environmental Protection Agency |
| IARC | International Agency for Research on Cancer |
| IDN | Identification Number |
| ISO | International Organization for Standardization |
| LETRU | Low Emission Transport Refrigeration Unit |
| LFE | Laminar Flow Element |
| MAE | Mechanical and Aerospace Engineering |
| MFC | Mass Flow Controller |
| NASA | National Aeronautics and Space Administration |
| NRTC | Nonroad Transient Cycle |
| ODP | Opti-Drive Plus |
| OM | Organic Matter |
| PAH | Polynuclear Aromatic Hydrocarbons |
| PM | Particulate Matter |
| RTD | Resistance Temperature Detector |
| SETC | Small Engine Test Cell |
| SEE | Standard Estimate of Error |
| SI | Spark Ignition |
| SOF | Soluble Organic Fraction |
| THC | Total Hydrocarbon |

| | |
|---|---|
| TRU | Transport Refrigeration Unit |
| TRU ATCM | Transport Refrigeration Unit Air Toxic Control Measure |
| ULETRU | Ultra Low Emission Transport Refrigeration Unit |
| VDECS | Verified Diesel Emission Control Strategy |
| WVU | West Virginia University |
| $B$ | Laminar Flow Element Constant |
| $b$ | Offset Constant for Venturi Calibration |
| $C$ | Laminar Flow Element Constant |
| CO | Carbon Monoxide |
| $CO_2$ | Carbon Dioxide |
| $CH_4$ | Methane |
| $D$ | Diameter |
| $Err$ | Overall Uncertainty Propagation throughout the Final Calculation |
| $f$ | Function |
| HC | Hydrocarbon |
| $H_2O$ | Water |
| $H_2SO_4$ | Hydrogen Sulfate |
| $k$ | Linear Multiplication Constant for Venturi Calibration |
| $N$ | Engine Speed |
| NO | Nitric Oxide |
| $NO_2$ | Nitrogen Dioxide |
| $NO_x$ | Oxides of Nitrogen |
| $P$ | Pressure |
| $Q$ | Volume Flow Rate |
| Re | Reynolds Number |
| $T$ | Temperature |
| $u$ | Associated Error of a Component Used in a Final Calculation |
| $\Delta$ | Delta |
| $\partial$ | Partial Differential |
| $\mu$ | Kinematic Viscosity |
| $\tau$ | Engine Torque |
| $\nu$ | Velocity |

| | |
|---|---|
| $\rho$ | Density |
| *1* | Represents the Intake Point within a System |
| *Abs.* | Absolute |
| *Actual* | Pertaining to the Actual System Flow |
| *Desired* | Desired Output |
| *Ex* | Pertaining to the Engine Exhaust |
| *FC* | Fuel Consumption |
| *Flow* | Specific to the System Flow |
| *Input* | User Input |
| *Int.* | Intake |
| *MFC* | Mass Flow Controller |
| *Mix* | Pertaining to the Dilution Tunnel Mixture |
| *SDA* | Secondary Dilution Air |
| *Std* | Pertaining to the Flow in Terms of Standard Conditions |
| *Venturi* | Pertaining to the Flow Measured Through the Subsonic Venturi |

# Chapter 1: Introduction

# 1 Introduction

## 1.1 Introduction

In recent years there has been an increasing concern with regard to the relationship between diesel particulate matter (PM) emissions and environmental pollution, as well as public health. PM was recognized by the California Air Resources Board (CARB) as a toxic air contaminant (TAC) in 1998 [1], and since then regulations have been placed on large on-and-off-road diesel engines to decrease the amount of PM emitted. There exist now limitations on the emissions of small mobile and stationary diesel engines, including engines operating transportation refrigeration units (TRUs), TRU generator sets and auxiliary power units (APUs). This genre of engines provide electrical power for small operations, or run compressors for refrigerating or heating climate controlled storage spaces on trailers and rail cars transporting temperature sensitive products, usually ranging from 9 to 36 horsepower (hp) [2].

President Obama has directed a presidential memorandum that would allow California, as well as other states, the right to set more stringent state-wide standards for vehicle emissions for light duty trucks and automobiles [3]. This comes in response to California's request to the Environmental Protection Agency (EPA) to grant California a waiver within the Clean Air Act to allow the state to set more demanding emissions standards ahead of the national schedule [3]. With these new directives making their way through the legislative system, these standards will come to envelope the emissions of TRU, APU, and similar small diesel engines, as well to help protect the surrounding environment and the workers that are constantly in the area of operating units.

CARB's initiative includes the implementation of strict regulations on any TRU that operates within the state of California, regardless of its origin under the Transportation Refrigeration Unit Airborne Toxic Control Measure (TRU ATCM) [2]. As of January 9, 2009, (CARB) has been approved by the Environmental Protection Agency (EPA) for the waiver which would allow it to fully enforce these new TRU regulations with serious consequences for owners and operators who do not conform. CARB is also requiring facility reports, detailing the size and type of facility, along with the amount of TRU activity taking place. These facility reports were due January 31, 2006, and is now requiring initial operator reports for TRUs and TRU gensets, as well as identification numbers (IDNs) for all TRUs operating in California as of January 31, 2009 [1].

## 1.2 Why Build a New test Facility at WVU?

With these new regulations, there will be an increased need for the ability to perform emissions tests on small diesel engines, such as TRUs or APUs, and even similar spark ignition engines as well. At this time, the majority of the capabilities of West Virginia University's (WVU's) diesel engine emissions testing facilities lie within the realm of large (ranging from 100 horsepower to larger than 300 hp) on-and-off-road diesel engines, with the exception of the eddy-current dynamometer which has been used in recent times for testing small engines. These larger engine facilities are not set up to perform tests on small engines similar to that of a TRU, and due to some reliability issues, scheduling issues, and general wear and tear, there has been a push to reduce the usage CAFEE's existing eddy current dynamometer for small engine testing. This created the need for a new laboratory capable of testing this lower power engine range. This thesis document describes the development process, as well as the commissioning of a new laboratory for small engine testing set within the CAFEE annex facility in the Morgantown

Industrial Park in Westover, WV. Construction of this lab will give WVU the ability to perform emissions tests on smaller diesel engines of up to 40 horsepower including related after-treatment devices such as Diesel Particulate Filters (DPFs), and Diesel Oxidation Catalysts (DOCs). For the remainder of this document the Small Engine Test Cell will be referred to using the abbreviation (SETC).

# Chapter 2: Literature Review

# 2 Literature Review

## 2.1 What is a TRU?

A Transport Refrigeration Unit (TRU) is a device used to refrigerate the storage space for products which require a temperature controlled environment during transport, such as fruits, vegetables, pharmaceuticals, beverages, and other day-to-day consumables. TRUs can be found on ocean shipping containers, rail cars, road truck trailers, and airplanes [4]. TRUs contain diesel engines ranging from 10 to 50 hp which operate a compressor used to facilitate temperature management of the cargo containment area. The TRU is required to keep the container goods at their specific temperature despite the ambient conditions outside translating to the TRU having capabilities to cool goods in warm climates and to keep goods warm in colder temperatures [4]. Operation of a normal TRU consists of two phases. The first being referred to as "pull down" in which a container needs to be cooled from the ambient temperature to the shipment's specified temperature, which for most typical TRUs takes anywhere from ten to thirty minutes. The second phase of TRU operation is maintaining this setpoint temperature despite the outside environment conditions [4]. The TRU must also deal with a fluctuation in thermal loading caused by opening and closing of the container doorway when loading and unloading shipments. This increases the size requirements for most TRUs in proportion to the volume to be cooled [5].

The TRU came into existence in the 1930s as demand and need for long distance transport of meat, poultry, and dairy products was vastly increasing. The first model was developed by the U.S. Thermo Control Company, which exists today as Thermo King. Though this early model was large, bulky, and mounted below the trailer, it was successful, and after

several more iterations, a sleek front mount unit was available by the 1940s [6]. Today, sophisticated refrigeration units with precise temperature control systems allow people of all areas to enjoy food from far away, such as tropical foods in the winter, or even ice cream from another country. Currently, more than three quarters of food produced, packaged, stored, and shipped within the United States is under refrigeration, contributing to a frozen foods industry of annual sales in excess of $40 billion dollars. Refrigerated transport is not only limited to food items, but extends even to flowers, pharmaceuticals, and even photographic film [6]. An image of a typical TRU manufactured by Thermo King can be found in Figure 1.


**Figure 1: Thermo King SB-400 trailer refrigeration unit [7].**

## 2.2 Why is it Important to Measure TRU Emissions?

In 2004 the California Air Resources Board (CARB) approved the TRU Airborne Toxic Control Measure (TRU ATCM) for In-Use Diesel-Fueled Transport Refrigeration Units (TRU) and TRU Generator Sets, and Facilities Where TRUs Operate [1]. This measure requires all TRU or TRU generator sets that operate in California, regardless of base location, to meet documented in-use performance standards which were phased in as of December 31, 2008 [1]. The design of the TRU ATCM was set up to be a phased approach spanning the next 15 years to reduce particulate matter (PM) emissions from in-use TRU and TRU generator set engines operating within the borders of California [1]. Given California's current concentration on TRUs and its

history as a bellwether state, one can certainly expect to see similar regulations occurring in other states in the near future.

## 2.3 What is an APU?

APU is the an acronym for Auxiliary Power Unit which covers a broad range of engine types from that of a typical household generator to airplane power sources, and are approximately 10hp in size. APUs are used to provide power for system accessories in lieu of a larger engine in an effort to reduce fuel consumption, as well as produce lower emissions. When traveling long distances, requiring overnight stops truck drivers rely on their cabin accessories to maintain comfortable cabin temperatures, and to supply electricity for their entertainment devices. In the past, while the driver was parked for the night, the large diesel engine was left idling to provide power to run climate control and power systems within the cabin, as well as to protect the engine during cold weather conditions [8]. This led to large amounts of excess diesel emissions, as well as wasted fuel consumption. APUs allow the truck driver the full range of comforts without the use of the main engine or restricting where the truck must stop [9]. An image of a typical APU system is shown below in Figure 2.

**Figure 2: Photograph of typical APU system [8].**

## 2.4 What is Particulate Matter?

With the use of a diesel fueled internal combustion engine to drive the compressor, TRUs are a significant source of particulate matter (PM) exhaust emissions. Particulate matter expelled from a diesel engine holds no specific definition as a substance of its own, however is described as that of a complex mixture of varying chemical composition and physical properties [10]. Diesel engine exhaust emissions are heavily dependent upon the combustion characteristics of the operating engine such as fuel injection system, engine control systems, and intake and combustion chamber design [11]. The properties of diesel PM are dependent upon many different factors including fuel properties, operating conditions, lubricating oil consumption, and engine technology. Particulate matter is formed within the diesel combustion cycle at temperatures between 1000 and 2800 Kelvin and pressures of between 50 to 100 atmospheres [12]. For older technology engines the composition of Diesel PM (DPM) is mainly elemental carbon particles which agglomerate with other species forming complex structures [13].

These diesel particulate structures are categorized as a mixture of two different modes of formation, the first being nuclei mode, and the second being accumulation mode. Particles considered to be of nuclei mode are small, ranging from 0.007 to 0.04 μm in diameter, and represent only a few percent of the PM mass, yet comprise approximately 90% of the total particle number [13]. It is at this stage when the soot precursors such as unsaturated hydrocarbons, acetylenes, and polynuclear aromatic hydrocarbons (PAH) begin to form, and the condensation of these components become the first recognizable soot material [12].

Agglomeration of primary carbon particles and other solid materials forms the accumulation mode particles, which exist as a combination of solid carbon mixed with condensed heavy hydrocarbons, as well as, sulfur compounds, metallic ash, etc. This mode is

also referred to as particle growth, and includes surface growth, coagulations, and aggregation of the smaller spherules [12]. Accumulation mode particles represent the majority of PM mass and have a diameter ranging between 0.04 and 1 µm, with a high concentration of particles having diameters between 0.1 and 0.2 µm [13]. Figure 3 below gives an image interpretation of the structures of the Nuclei and Accumulation mode particles. It is important here to note that with agglomerated particles spherical diameter is only an approximation of size, as these particles tend to form chain like, non-spherical structures.

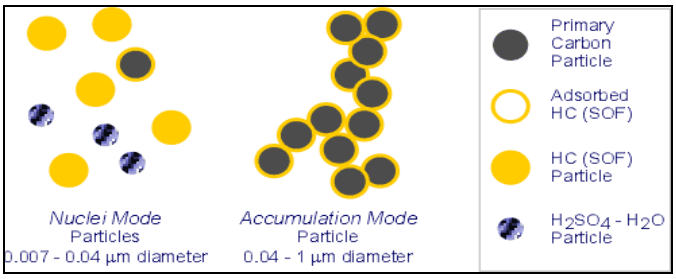


**Figure 3: Representation of Diesel Particulate Matter, [9].**

## 2.5 Environmental Concerns Associated With Diesel Exhaust From TRUs and APU Engines.

Despite being more fuel efficient, and as a result, producing lower amounts of the greenhouse gas $CO_2$ than spark ignition gasoline engines, diesel engines emit significant amounts of PM. Long-Haul freight trucks alone produce approximately 5,000 tons of particulate matter each year, 12 tons per year in West Virginia, and 45 tons per year resulting from truck traffic in Virginia [8]. Increased localized air concentrations of diesel particulate matter degrade visibility, and despite accounting for roughly 5% of on road vehicles in the US, diesel engine exhaust contributes as much as 75% of the observable particulate matter in metropolitan areas [14]. A flow chart, reproduced from Lloyd and Cackette [15], and shown below in Figure 4

details the scope of the environmental implications associated with the production and use of diesel engines.

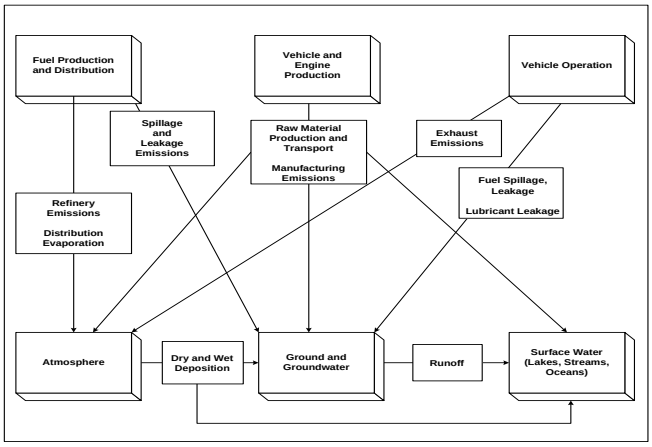


**Figure 4: Environmental effects associated with the production and operation of diesel engines, [17]**

Some studies, such as that performed by Dr. Mark Z. Jacobson of the Civil and Environmental Engineering Department of Stanford University suggest that diesel particulate black carbon, and the remaining organic matter (OM) related to "soot" may be a significant contributor to global warming. According to Jacobson, the soot produced in diesel combustion has a greater global warming effect per unit mass than carbon dioxide. The difference is that particulate matter has a significantly shorter atmospheric lifetime, on a scale of months, as compared to the 50 to 200 years which carbon dioxide remains in the atmosphere. Jacobson suggests that while control of carbon black from the combustion of fossil fuels alone will not eliminate long term global warming, which requires a reduction in overall greenhouse gas emissions, removal of soot and its related organic particulate should have a faster effect on slowing the progress of global warming [16]. Jacobson's study used a global climate model which accounted for 12 different effects of aerosol particles, including self feedback effects, photochemistry effects, particle effects, and others which are further described in his report, on

global climate. Jacobson's model is referred to as the Gas, Aerosol, Transport, Radiation, General Circulation, and Mesoscale Meteorological model (GATOR-GCMM) [17]. Three simulations were performed on a "with and without" basis over a span of six years. The first operated with current levels of anthropogenic $CO_2$, the second using current levels of anthropogenic $CH_4$, and the third operating with emitted fossil fuel black carbon (BC) + organic matter (OM) [17].

Based on the results, Jacobson suggests that reduction in the emission of fossil fuel BC + OM will slow the progress of global warming more than any reduction in the emissions of $CO_2$ or $CH_4$ for a specific period [17]. For example, if all fossil fuel BC + OM and anthropogenic $CO_2$ or $CH_4$ emissions were eliminated together, that period would be 25 to 100 years [17]. As net global warming can be attributed to greenhouse gases plus fossil fuel BC + OM emissions, minus some cooling from other anthropogenic particles, Jacobson states that eliminating all fossil fuel BC + OM could eliminate 20 to 45% of the net global warming [17]. Jacobson goes on to suggest that diesel cars operating under the most recent U.S. and E.U. particulate standards may warm the climate per distance driven more than gasoline vehicles, and that fuel and tax laws that favor diesels may in fact promote global warming [17]. Jacobson also mentions in another study on the radiative heating forcing of carbon black that "*the magnitude of the direct radiative forcing from black carbon itself exceeds that due to $CH_4$*" suggesting that black carbon may be the second most important component of global warming after $CO_2$ in terms of direct forcing [18]."

In a study performed by NASA, concentrating mostly in the Northern Hemisphere and Arctic areas, describing how soot components, from the burning of fossil fuels, such as carbon black were found to cause a reduction in the albedo, or sunlight reflectivity, of snow and ice [19].

As soot material falls from the atmosphere, whether within the air, or attached to snow flakes, there is a mixing of the carbon black and other aerosols with the snow. These soot particles mixed within the snow darken the overall visible appearance of the snow, and absorb solar radiation, lessening the reflective properties of the snow or ice, and leading to premature and advanced melting. The decreased albedo and increased melt rate contributes to a global warming positive feedback system that only then furthers melt rate, and decreases albedo with added snow or ice loss. Similarly, carbon black particulates within the atmosphere warm the air, causing snow to melt as it falls, reducing snow cover and further reducing albedo [19]. Hansen states that the soot effect on snow albedo may be responsible for a significant amount of global warming [19]. Heavy metals, PAHs, and dioxins associated with diesel particulate matter are also of significant environmental concern. These toxins can be transported long distances, are resistant to degradation, and are often found in high concentrations in many rural areas [20; 21]. Multiple other sources have described finding these DPM related toxins in lake sediments in Michigan, and Sweden [22; 23], as well as in German Forest Canopies [21].

## 2.6 Infrastructure-Related Concerns with Diesel Particulate Matter

Not only can diesel PM and its associated toxins be degrading to the environment and surrounding ecosystems, but they can also affect the more "man-made" aspects of our daily lives as well. The deposition of PM can cause considerable damage to the surfaces of buildings, tunnels, bridges, and historical landmarks [24, 25]. High concentrations of these pollutants can even weaken the protective film layer that many metals form to shield themselves against corrosion [26]. This effect of diesel particulate matter can come at a considerable cost for maintaining, repairing, and caring for these structures. A study performed in 1982 by Sawyer

Associates for the California Air Resources Board estimated that, for a hypothetical dieselization of 20% of the light-duty vehicles operating in California, an annual cost of $800,000,000 to households associated with damage from airborne particle soiling for diesel exhaust [27].

## 2.7 Health Concerns with Diesel Particulate Matter

Along with the environmental concerns with respect to PM, there are human health concerns as well. Much of the matter formed in the combustion of diesel fuel exists as fine and ultrafine particles, of about 2.5 microns in mean diameter, that are respirable, as they can avoid the biological defense mechanisms as they enter human respiratory system. This type of exposure can come from both road and non-road engines either directly or through aged particles existing in the atmosphere for extended periods of time [28]. Exposure to PM can affect human health in different ways depending upon exposure. Short term exposure effects often present themselves as eye, nose, throat, or lung irritation, as well as some instances of lightheadedness. Considerable evidence based on human epidemiological studies suggests that with chronic exposure, PM is a likely carcinogen, as these studies exhibit a link between the diesel engine exhaust and increases in lung cancer rates [28]. As of 1991, the International Agency For Research on Cancer (IARC), listed diesel engine exhaust, and its constituents, within their designation of "Group 2A" of probable carcinogens to humans [29].

The relation between chronic diesel PM exhaust exposure and increased cancer risk has been demonstrated in laboratory tests with rats by studies performed by the Diesel Working Group within the Health Effects Institute. It has been shown that rats, which were exposed to high concentrations of PM for 35 or more hours per week (2000 to 10,000 $\mu g/m^3$), had an increase in exposure dependent cases of both benign and malignant tumors within the lungs [30].

The Diesel Working Group does recommend caution in relating these finding to humans due to the lack of sufficient data, as well as possible species specific responses [30]. A study by the West Virginia University Center for Interdisciplinary Research in Cardiovascular Sciences gives results that provide a link between diesel engine particulate exhaust exposure and impaired vasoreactivity and diminished blood flow to certain bones in rats[31]. The study opens discussion to the idea that there is also concern that diesel particulate exhaust may affect the human cardiovascular system along with increasing cancer risk.

The concerns for health with TRU engines stem from the long periods of exposure during which workers involved with the shipment of refrigerated goods are exposed to diesel exhaust at the workplace. It is estimated that, on an eight hour average for trucking occupations, exposure levels can range from 1 to 100 $\mu g/m^3$, and epidemiologic evidence exists suggesting that there is an increase in lung cancer risk among occupations with this degree of exposure [30]. An article from the Sacramento Bee discusses the link between diesel soot and an increased death rate from heart disease of 49%, and a lung cancer death rate increase of 10% in truck drivers [32]. CARB has also stated that those most vulnerable, outside of ones with work-related exposure, are children who are young with still-developing lungs, and elderly with other serious health issues [33]. The genetic material DNA may also be at risk from diesel particulate matter. Some of the PAHs found in PM have been observed to damage DNA, as well as be absorbed into the bloodstream leading to cell and tissue damage [34]. One such contaminant of note is Benzene, which is a known leukemia causing agent can be found in both the gaseous and particulate matter forms of diesel exhaust [34].

## 2.8 What are the Regulations Introduced Concerning TRU and APU Engines?

As described earlier, the California Air Resources Board (CARB) has been working to lower emissions on vehicles and equipment operating within the borders of California. These regulations are now being implemented as CARB's TRU ATCM. This measure, which has been approved for enforcement by the EPA as of January 9th 2009, to reduce the PM emissions from in-use TRUs and TRU generator sets used to power electrically driven refrigerated shipping containers and trailers that are operated in California [2]. In order to comply with the TRU ATCM all owners and operators of TRUs within California must be using a certified engine meeting the applicable off-road and on-road emissions standards for all regulated pollutants, as well as the in-use PM performance standards described in Figure 5 and categorized based on engine horsepower.

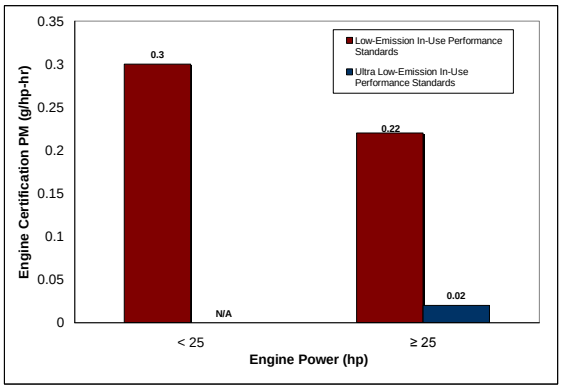


**Figure 5: CARB engine certification particulate matter levels. [2].**

As one can see from Figure 5, the CARB has set two levels of emissions requirements for TRUs, one being Low Emission TRU (LETRU) and the other Ultra Low Emission TRU (ULTRU). It is important to note that for the ultra low-emission in-use performance standards for engines rated at 25 horsepower or lower, there is no existing engine certification rating for

particulate matter. CARB and the EPA are currently evaluating Diesel Oxidation Catalyst (DOC) or filter-based standards for this range of horsepower rating that is to be ready in 2013 [2]. To clarify, the PM requirements are given in (g/bhp-hr) or, grams per brake-horsepower hour, which is a measure of the average emissions for a certain amount of work performed by the engine. Brake horsepower itself is the engine horsepower measured at the engine output shaft.

An owner/operator may also be compliant by equipping a non-certified engine with the appropriate required level of Verified Diesel Emissions Control Strategy (VDECS), which are listed in Table 1 [2]. VDECS refers to a means of emission control designed primarily for the reduction of PM emissions per the California Code of Regulations (CCR) Title 13 Sections 2700-2710, such as diesel particulate filters, diesel oxidation catalysts, fuel additives, alternative fuels, and combinations of these [2]. The PM reduction associated with the different VDECS levels is described below in Figure 6. It should be noted that Level 3 may be met with either greater than 85% PM reduction or a tested PM emission level of less than 0.01 g/bhp·hr [35].

**Table 1: VDECS for TRU engines based on horsepower range, [2].**

| In-Use Emission Category | Power Range (hp) | Engine Certification PM (g/bhp-hr) | Level of VDECS |
|---|---|---|---|
| Low Emission TRU | <25 | 0.3 | Level 2 |
| Ultra-Low Emission TRU | <25 | N/A | Level 3 |
| Low Emission TRU | ≥25 | 0.22 | Level 2 |
| Ultra-Low Emission TRU | ≥25 | 0.02 | Level 3 |

These criteria must have been met for all TRUs of 2001 and older model year (MY) by December 31, 2008 for LETRU, and by December 31, 2015 for ULETRU [2]. Engines of MY 2002 must meet the criteria for LETRU by December 31 2009, and ULETRU by December 31 2016, and engines of MY 2003 and later must meet the requirements of ULETRU by December 31 of the seventh year past the unit's model year, depending upon horsepower rating as described in Table 2 [2].

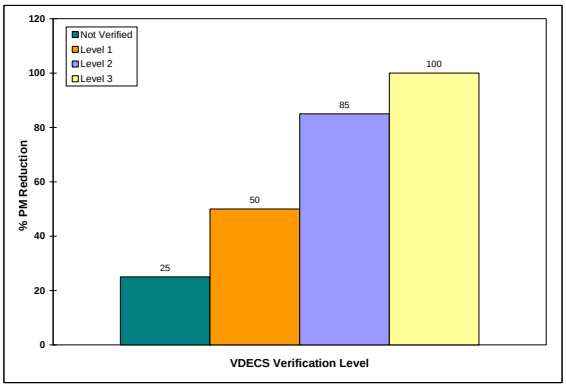


**Figure 6: Verified Diesel Emissions Control Strategy Verification Levels, [2].**

**Table 2: From the CARB Final Regulation Order, In-Use Compliance Dates [2]**

| MY | In-Use Compliance Year For TRU Engines Rated < 25 hp | | | | | | | | | | | | | |
|---|---|---|---|---|---|---|---|---|---|---|---|---|---|---|
| | '07 | '08 | '09 | '10 | '11 | '12 | '13 | '14 | '15 | '16 | '17 | '18 | '19 | '20 |
| ≤ 2001 | | L | L | L | L | L | L | L | U | U | U | U | U | U |
| 2002 | | | L | L | L | L | L | L | L | U | U | U | U | U |
| 2003 | | | | U | U | U | U | U | U | U | U | U | U | U |
| 2004 | | | | | U | U | U | U | U | U | U | U | U | U |
| 2005 | | | | | | U | U | U | U | U | U | U | U | U |
| 2006 | | | | | | | U | U | U | U | U | U | U | U |
| 2007 | | | | | | | | U | U | U | U | U | U | U |
| 2008 | | | | | | | | | U | U | U | U | U | U |
| 2009 | | | | | | | | | | U | U | U | U | U |
| 2010 | | | | | | | | | | | U | U | U | U |
| 2011 | | | | | | | | | | | | U | U | U |
| 2012 | | | | | | | | | | | | | U | U |
| 2013 | | | | | | | | | | | | | | U |

CARB is requiring that owners and operators keep records and reports in accordance to Subsection (f)(1) of the TRU ATCM which includes various information regarding the owner, make and model of the unit as well as the container it is equipped for [2].

With regard to APU engines, there seem to be few actual regulations in place, however there is a hint of policy on the matter beginning to emerge that will most likely further the use of APUs in the future. The EPA SmartWay Transportation Partnership mentions that some states have brushed the topic of anti-idling laws in an attempt to limit truck drivers from idling their engines for long periods of time at truck stops. SmartWay describes however that such a law would not only be difficult to enforce, but be unfair to implement when alternatives are not available [36]. It will also be difficult to change the behavior of truck drivers since idling is

necessary to provide comfort during resting times, however with the use of an APU engine, these comforts can be retained without the use of idling the primary engine [36].

## 2.9 Existing Diesel Exhaust Particulate Matter Emissions Control Systems

As previously stated, the PM produced in diesel engines is detrimental to both the environment, and human health. Reducing the amount of PM that is released to the atmosphere through the tail pipe is a major issue. Recently there has been quite a lot of advancment in diesel exhaust after treatment devices, and particulate matter control. The following subsections will outline several of these particulate control methods.

### *2.9.1 Diesel Oxidation Catalyst*

One particular method of reducing the output of PM is a Diesel Oxidation Catalyst (DOC). The DOC consists of a cylindrical tank plumbed in as part of the exhaust line which the exhaust gases flow through in lieu of a standard muffler [37]. Within the DOC is a honeycomb structure made of a ceramic material that is coated with a catalyst material. The catalytic layer is generally composed of metals, such as platinum or palladium. Exhaust gases travel through the exhaust line and through the catalyst and pollutants within the exhaust, such as CO and unburned fuel hydrocarbons, are oxidized upon the catalyst and emissions are reduced [38]. The following illustration in Figure 7 shows the various shapes and sizes of typical DOCs.

**Figure 7: Examples of typical Diesel Oxidation Catalyst units.**

Diesel Oxydation Catalysts can reduce CO emissions up to 40%, Hydrocarbon (HC) emissions up to 55%, and reduce PM between 35 and 50% [37,38]. Other studies show HC, and CO emission reduction efficiences of up to 80 and 90% [39]. DOCs have been observed to reduce soluble organic fractions at efficiencies between 80 and 90%. Reductions can vary with engine size, type, age, manufacturer, and operating conditions. [38]. DOCs can be retrofitted to existing diesel engines in the form of in-line muffler replacement, or add on control devices. DOC's vary in cost, and can range from $2,100 for a 275 horsepower engine to $20,000 for a 1,400 hp engine. In general, one can estimate about $12 per horsepower. A retrofit for a diesel engine is described by the EPA as, any technology that when applied to an existing system reduces the emissions beyond that which is currently required by EPA regulations upon certification [40]. A detailed list of retrofit systems, manufactures, and verification data can be found on the EPA and CARB websites.

### *2.9.2 Diesel Particulate Filter*

Another method of PM reduction is a Diesel Particulate Filter (DPF). Similar to a DOC, a DPF unit contains an inner honeycomb structure and the exhaust gases pass through the internals of the DPF and a majority of PM is captured and prevented from entering atmosphere [12]. A depiction of the internals of a DPF can be found in Figure 8.

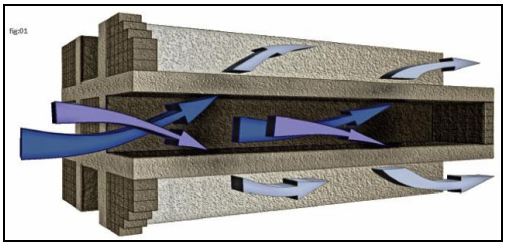

**Figure 8: PM is captured from the exhaust flow by a DPF [41].**

As PM accumulates inside a DPF, the system requires regeneration to remove this PM build up. DPF systems operate with either a active or passive regeneration to rid the internal structure of the captured PM, converting it to $CO_2$. Active regenerative filters contain either electrical heaters, or use fuel burners, or require engine modification to increase the exhaust temperatures. In a fuel burner regeneration system, once the PM has built up to a certain point, a sensor communicates with the system's computer, which will then control the fuel injection to allow unburned fuel to enter the filter in specific amounts. Oxygen, containing exhaust gas is also introduced to aid in the combustion of the collected PM[12]. This unburned fuel will flare and increase the temperature of the particulate filter enough to reach the ignition point and burn off the soot that has collected upon the filter surface. This active regeneration process must be carefully controlled in order to prevent excessively high temperatures that may damage the filter itself [12]. Figure 9 which follows, shows an image of a DPF unit installed on a Fored F-250 Super Duty Diesel truck.

**Figure 9: Diesel Particulate Filter, as installed in the exhaust system of a Ford F-250 Super Duty Diesel truck [42].**

Passive regeneration DPF modules are catalyst based, and contain a catalytic layer, much like that of a DOC. These catalyst-layered DPF units operate at lower temperatures. Problems with regenerative heaters lie in the high power demand of the heaters, or the high fuel consumption of the fuel burners. Diesel Particulate Filters have impressive emissions reduction

results. CO can be reduced between 60 and 90%, likewise PM and HC have been observed to have been reduced between 60 and 95%. As with the DOC, these results can vary with manufacturer,  and operating conditions [37]. DPF units are mostly used in light-duty automobile diesel engines, and transit buses. Heavier duty diesel engines have a greater PM load, which leads to problems with running a DPF [12]. It should also be mentioned that DPF units have little effect on total NOx levels [40]. DPF units must be maintained and periodically cleaned as overtime there is some PM that will not burn off during regeneration. Ash also accumulates on the filter due to inorganic calcium sulfate and zinc phosphate stemming from the engine lubrication oil [40]. Directing compressed air through the filter itself will work, as well as, typical cleaning, or returning to the manufacturer for cleaning. This must be done to prevent engine problems related to the increased back pressure caused by the clogging of the filter. DPF units are more expensive than DOCs, and range anywhere from $5,000 to $8,000 installed, and also encur maintenance costs. With the advent of this new test cell, the WVU CAFEE group will have the capability to perform cycle testing on similar DPF and DOC units.

## 2.10 Current Emissions Testing and Research Involving TRUs and Other Small Off-Road Engines

### *2.10.1 University of California, Davis TRU Emission Testing – 2007*

At this time, there is a relatively light amount of research being done with respect to emissions testing and verification of TRU engines. However, with the California requirements coming into place, it is expected that there will be significantly more research being performed in this area in the future. There has been one group, as of late, within the Mechanical and Aerospace Engineering department of the University of California at Davis, producing documentation and results regarding the testing of TRU engines. In one study, Mader et. al.

performed a series of tests in order to characterize the load and emissions of TRU engines in the field [5]. To perform this type of characterization, the gases $NO_x$, $CO_2$, CO, and $O_2$ were measured in order to meet the desired goal of quantifying the major emissions produced by TRUs over the range of their working conditions, although PM was not measured in this specific study [5]. Three models of TRU were tested; a Supra 722, Supra 744, and Extra XT, with the Supra 744 operating with a Kubota CT3-44 TriVortex three cylinder diesel engine of 719 cubic centimeters, the Supra 722 being a slightly older version of the same and the Extra XT used a Kubota 1.9 liter four cylinder diesel [5]. Testing was performed during the cold weather months of December and January at different temperatures and humidities, as well as spring months of March and April with temperatures between 65º and 70º F, and then finally during late June and July with temperatures above 90º F [5].

The results from these tests found that the engines were not a significant source of CO, as compared to similar SI engines, at levels being approximately 125 ppm [5]. The Supra 744 and Extra XT were found to produce $NO_x$ at concentrations valuing 400 ppm and over 500 ppm respectively, while maximum levels for each, which came about while the units were "pulling down" the refrigerated space to the setpoint temperature of 38º F, were found to be 22.5 g/hr and 57 g/hr respectively, which far exceed that of comparable SI engines [5]. As a result of these tests Mader concluded that CO emission is a minor concern with TRU emissions, but $NO_x$ is where future TRU testing concerns should fall. Mader gives a final value for $NO_x$ from these tests in grams per kW of cooling between the range of 3.6 g/kW·hr to 5.15 g/kW·hr depending upon the model tested and the time of year [5]. Despite not performing PM sampling on these units during testing, this report has shown that there is a significant source of environmentally

harmful substances emitted from TRU engines, and furthers the notion that there is quite a bit of more work to be done in this area.

### *2.10.2 YANMAR Co., Ltd. – 2005*

A Japanese study was conducted to quantify PM emissions for off-road diesel engines with both steady state and transient cycle testing [43]. Experiments were conducted using a filter sampling method as well as an Engine Exhaust Particle Sizer (EEPS). Emissions tests were operated with the steady state C1 mode and the Non-Road Transient Test Cycle (NRTC) using a four cylinder direct injection 44 horsepower diesel engine.

During steady state testing PM emissions were found to increase with engine speed, as well as with load. Total hydrocarbon (THC) emissions and percentage of SOF were found to increase at high engine speed and low load operations. Particles of 50 to 60 nm in diameter were found to peak in concentration at rated speed, and smaller particles on the scale of 10 to 20 nm were found to be emitted mostly at light loads [43].

Under transient operation it was found that fine particles are high in concentration where as the concentration of larger particles tends to be lower. The study suggests that this may be a result of more frequent low load operation with the transient cycle [43].

### *2.10.3 HORIBA Ltd. – 2007*

A group of researchers with HORIBA, Ltd. in Japan performed a study on the solid and volatile particle emissions created by a small off-road diesel engine. This study was conducted as a result of recent regulations by the European Particle Measurement Program (PMP) for light-duty diesel vehicle exhaust particle number measurement for on-road diesel engines, recommending that number concentration of solid particles should be measured after eliminating

volatile particles from the exhaust gas. Under the assumption that these new regulations will soon extend to small off-road engines as well, HORIBA went forward with this study [44].

The testing was performed using a single cylinder, air cooled, 2.8 kW direct injection diesel engine from an electrical generator set. Exhaust from the engine was sampled and diluted with a dilution ratio of 4 under room temperature to ensure that a large number of volatile particles would be formed. A particle number counting system was developed for the project, which included a cycling, a first stage diluter, an evaporation unit (EU), used to evaporate volatile particles within the exhaust, and a second stage diluter. The generator engine was operated at different conditions which included idle, 100 W, 200 W, and 400 W load, all while maintaining a constant speed of 3600 rpm [44].

The study concluded that with small off-road diesel engines, solid particle number emissions increases with increasing engine load, while volatile particle number decreases, as well as that the volatile to solid particle ratio decreases with increase in load and increase in dilution air temperature [44].

## 2.11 Conclusion

This chapter has introduced a significant amount of background material describing small diesel engines and their emissions characteristics, specifically with regard to PM. With the recent legislation concentration towards this genre of diesel engine, and based on material presented above, a new small engine testing facility was developed within the WVU CAFEE in order to facilitate emissions testing of small engines.

# Chapter 3: Small Engine Test Cell System Development and Setup

# 3 Small Engine Test Cell System Development and Setup

## 3.1 Introduction

During the initial stages of the project, there was much deliberation as to how the lab would be setup, what its location would be, as well as what type of work should be expected for the labs future. Final criteria called for a facility capable of performing emissions tests on engines at or below 40 horsepower, with the ability to be operated with all current CAFEE emissions testing equipment, as well as have the capacity for future upsizing. Specific aspects of the new facility's build are described within the following sections.

## 3.2 CAFEE Mobile Lab Annex in Morgantown Industrial Park

The test cell, which became dubbed as the Small Engine Test Cell (SETC) was built within the CAFEE mobile lab annex located within the Morgantown Industrial Park in Westover, WV. This facility houses CAFEE's mobile emissions testing equipment and also has a separate test cell room, which was the designated new home for the SETC. It is important to note that, while the lab was initially being developed in the annex test cell, the equipment will have the capability to be mobile. This will allow the system to be transported to and from the CAFEE Engine and Emissions Research Laboratory (EERL) located on the WVU Evansdale campus if necessary.

## 3.3 Test Cell Development

### *3.3.1 Test Cell Cooling System*

The cooling system for the SETC was designed to operate with a closed loop water system. The intent of this layout was to reduce the amount of city water used during testing to

decrease cost. Heat generated by the engine, as well as generated by the immersion heater load bank, was removed by  cold water loops which circulated from a stainless steel storage tank located outside the lab room. Electricity generated by the electric motor dynamometer was dissipated to heat via a Chromalox Immersion Heater resistor load bank. This load bank was mounted within a second stainless steel storage tank and was also set outside of the lab room.

### *3.3.2 Water Supply Tank*

The stainless steel water storage tank was designed based on a similar tank located within the EERL. The tank was of rectangular shape with dimensions of 3 ft long by 3 ft tall and 14 inches wide which amounts to a 78 gallon capacity when full, and was self supported. An image of the tank as it was designed is shown in Figure 10.

**Figure 10: Stainless steel system water supply tank.**

### *3.3.3 Immersion Heater Tank*

A similar stainless steel tank was constructed to house the Chromalox immersion heater resistor bank and the water which will absorb the heat produced by the copper resistors of the heater. This tank was 2 ft tall by 14 inches wide by 6 ft long with a 170 gallon capacity when full and was also self supported. The front of the tank body had a collar and flange attached in order to mount the heater body within the tank. The mounting flange was designed based on the

immersion heater's own connection with drawing schematics provided by Chromalox. An image of the heater tank including the mounted immersion heater is shown in Figure 11.

**Figure 11: Immersion heater housing tank.**

### *3.3.4 Chromalox Immersion Heater*

A Chromalox immersion heater within the tank used a series of copper rods to dissipate the electrical energy, produced by the dynamometer motor, to the water contained within the tank. This particular unit was capable of dissipating 150 kW of electrical energy, which was the equivalent of about 200 hp and was significantly more than the current lab setup produced A series of wires, running from the "BR" and "POS" contact points on the bottom of the Invertek drive unit, delivered the absorbed electrical energy to the immersion heater. These wires branched from the Invertek drive unit by two large terminal blocks housed within an electrical enclosure mounted on the wall beside the drive unit. This is shown in Figure 12.

**Figure 12: Terminal blocks splitting the energy from the Invertek drive unit to the immersion heater.**

The bulk head of the immersion heater where the connection points were made was placed within a NEMA 12 electrical enclosure to protect the terminal points from the weather. An image of this can be found in Figure 13 below.

**Figure 13: Chromalox immersion heater within tank.**

### *3.3.5 Engine Coolant Surge Tank and Radiator*

A design for an engine coolant surge tank was made based on existing surge tanks within the EERL as well as at Westover. This stainless steel tank served as a storage tank for engine coolant. The tank itself was 24 inches tall by 6 inches square with a capacity of 3 gallons when full and was constructed with inlet and outlet pipe nipples, as well as a site tube allowing the user to see the level of coolant within. An image of the surge tank is shown below in Figure 14.

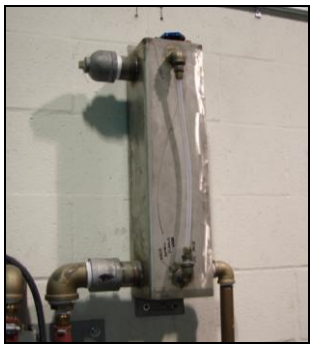

**Figure 14: Wall mounted coolant surge tank**

It was necessary to perform a pressure test on the coolant surge tank to show that there were no leaks and that the cap had sealed properly. This test was performed using pressurized

water available at the Westover facility. The water pressure was set with a pressure regulator at 20 psi, and a water hose was connected to the sealed tank. The pressurized water was allowed to fill the tank and begin placing pressure on the tank walls. After all initial leaks were sealed; the surge tank successfully maintained pressure, until the pressure cap opened at 16 psi.

### *3.3.6 Heat Exchangers*

Two large cross flow flat plate heat exchangers were added to the system that were capable of the cooling needs for the small engines that will be tested on the current laboratory setup, as well as possible larger engines in the future. These heat exchangers were purchased through the McMaster-Carr online catalog, are copper brazed and are designed for a cooling capacity of 1,239,00 Btu/hr. A steel mounting bracket was fabricated to allow for mounting of the two heat exchangers side by side on the wall. An identical unit was purchased to be used for the immersion heater coolant loop as well. An image of the heat exchangers mounted to the test cell wall is shown below in Figure 15.

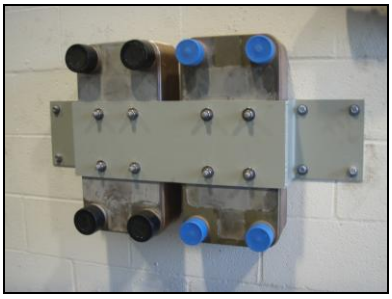

**Figure 15: Wall-mounted flat plate heat exchangers.**

### *3.3.7 Water Tank Radiator*

A large capacity six row radiator was installed to dissipate heat from the water within the main reservoir during engine testing. This unit was mounted outside of the test cell along with the reservoir and immersion heater tanks. This radiator is shown in Figure 16.

**Figure 16: Freightliner radiator to be used for rejecting heat generated within the main water tank during testing.**

Some time was spent in an attempt to size an adequate fan for this radiator, however it was difficult to determine exactly what would be needed based on the lack of information as to what temperatures the water within the tank will actually see. Due to insufficient funding at the time, no dedicated high powered fan was installed. During testing, a rolling industrial fan was used to force air through the radiator. It is the author's suggestion that once adequate funding is available, an appropriate fan should be purchased that will be dedicated to this system.

### *3.3.8 Concrete Pad*

A concrete pad was poured and finished outside of the small engine lab test cell bay for mounting of external items such as the immersion heater tank, water storage tank, and cooling radiator. The equipment and concrete pad can be viewed in the following Figure 17.

**Figure 17: New concrete pad and system cooling equipment.**

### *3.3.9 Water Pumps*

Four pumps were installed for the system, three centrifugal pumps to pump cold water from the storage tank outside through the two heat exchangers as well as the radiator system to cool the storage tank supply. The centrifugal pumps for the cold side application were purchased with 1 hp motors and were capable of 61 gal/min at 20 ft of head. A Grundfos hot water circulating pump was installed to pump hot water from the immersion heater load bank tank through the second flat plate heat exchanger.

## 3.4 Fuel Conditioning Box

A fuel conditioning box was built by MAE graduate students, shown in the following Figure 18, for this new lab. This box was based on a similar unit within the EERL and its purpose was to maintain fuel temperature during testing, as well as weigh the fuel for fuel consumption measurement. The box operated by using two separate small flat plate heat exchangers, one for the cold water loop, and one for a hot water loop. Solenoids opened and allowed hot or cold water to flow through to control the temperature of the fuel. The system was set to attempt to keep the fuel at 95 ºF.

**Figure 18: Fuel conditioning and weighing box for small engine test cell.**

Due to a lack of hot water available at the Westover facility, it was necessary to construct a small electric, tank-less water heater system for the hot side heat exchanger within the box. During the testing that was completed, the fuel conditioning box was not included within the test setup as certain aspects of the box, such as the water temperature control system, remain to be completed. Detailed schematics of the water and fuel flow, as well as the internal electrical components are given in the appendix of this document.

## 3.5 Electrical Work

Electrical power was installed within the test cell area by a local contractor. Other electrical equipment was installed by CAFEE staff. These items include a 480 volt transformer, and all wiring from the motor controller to the power box, as well as from the motor itself. Other electrical components consisted of power cables between the Invertek drive unit and the dynamometer motor, data cables between the Invertek and DYN-LOC and DTC-1 setup, wires connecting the Invertek to the immersion heater load bank, as well as power cables to engine components.

## 3.6 Dilution Air Blower

The existing blower units available within CAFEE were of too large for the small engine lab. A new small blower was needed with the capabilities of pulling air through the dilution tunnel at flow rates ranging from 250 to 1,000 scfm. The unit was purchased through P.F. Sherman Company in Pittsburgh, PA based on quotation 103239 dated 14 September 2007. The blower was a Cincinnati Fan model RBE-9 with a 7 ½ hp Baldor variable frequency drive electric motor. An image of the blower as delivered is shown below in Figure 19.


**Figure 19: Cincinnati Blower model RBE-9 used to pull dilution air/exhaust mixture through the dilution tunnel.**

## 3.7 Mobile Dilution Tunnel System

The new laboratory can be operated with existing CAFEE emissions testing equipment. However, a separate Continuous Volume Sampling (CVS) system would be needed to handle the lower flow rates of the small engines and small blower unit. A CVS system is necessary for dilute emissions testing in order to measure, on a continuous basis, the dilution air and exhaust mixture volume flow rate through the system. A separate section containing a smaller throat venturi will need to be in place during testing with the SETC. This CVS equipment has been fabricated and is ready to be mounted in place when needed.

The Code of Federal Regulations (CFR) of the Environmental Protection Agency (EPA) documentation per section 1065.130 states that the primary dilution tunnel shall be small enough in diameter to cause turbulent flow of the diluted exhaust to create proper mixing [45]. To achieve this mixing, the Reynolds number within the primary dilution tunnel was required to be greater than 4000. Based on a flow rate of 250 $ft^3$/min, which is towards the lower end of the flow rate spectrum for the purposes of the small engine lab, and an approximate temperature value of 300 ºF, for the 18 inch diameter dilution tunnel used, the Reynolds number is 11,528, which is well above the required 4000. The existing tunnel within the ’07 trailer will provide adequate mixing of the exhaust and dilution air for the flow rates that will be seen when testing

with the new Small Engine Test Cell. The process through which this calculation was achieved is based on Equation 1.

$$\mathrm{Re} = \frac{\rho v D}{\mu} \qquad \text{Equation 1}$$

Where,

**ρ** = the density of the dilution air/exhaust mixture in (slugs/ft$^3$) (kg/m$^3$)

***v*** = the velocity of the dilution air/exhaust mixture in (ft/sec) (m/s)

***D*** = the diameter of the primary dilution tunnel in (ft) (m)

**μ** = the viscosity of the dilution air/exhaust mixture in (lb-sec/ft$^2$) (kg-s/m$^2$)

The mixture at 300 ºF can be approximated with the density and viscosity of air alone, with values of 1.62e$^{-3}$ slugs/ft$^3$ and 4.97e$^{-7}$ lb-sec/ft$^2$ respectively. Velocity of the mixture was calculated based on the flow and area of the tunnel with Equation 2.

$$v = \frac{\dot{Q}_{Mix}}{A} \qquad \text{Equation 2}$$

Where,

$\dot{Q}_{Mix}$ = the flow rate of the dilution air and exhaust mixture through the tunnel in (ft$^3$/sec) (m$^3$/s)

***A*** = the cross sectional area of the tunnel in (ft$^2$) (m$^2$)

## 3.8 Small Engine Lab Dilution Tunnel Venturi

Due to the lower flow rates of the dilute system during testing with the small engine lab, a venturi designed for a lower flow system was required as the critical component of the CVS system to measure the flow rate of the dilution air and exhaust gas mixture. An existing venturi which was previously used for the Mobile Emissions Measurement System (MEMS) was allocated for use with the small engine lab. This venturi was developed by Flow-Dyne Engineering, Inc. in Ft. Worth, Texas with a throat size of 3.415 inches and is designed for flow rates of approximately 800 scfm and lower. Figure 20 provides an image of the separate components necessary to mount the venturi as part of the CVS system.

**Figure 20: SETC CVS system parts.**

## 3.9 Dynamometer and Control Equipment

### *3.9.1 Dynamometer*

To measure speed and torque of the engine during performing emissions tests, a dynamometer was required for the SETC. The dynamometer setup of the SETC was a system consisting of a 40 hp Reliance electric motor used to apply load to the test engine, and an Invertek Opti-Drive Plus to serve as the dynamometer controller. Figure 21 illustrates the

Reliance motor used as the dynamometer for the lab. Detailed dynamometer motor specification as well as the torque curve for the motor can be found in Table A - 1.

**Figure 21: 40 horsepower A/C motor used for the SETC dynamometer.**

### *3.9.2 DyneSystems, Inc. DTC-1*

Engine fuel rack control for the small engine lab was performed through the DyneSystems, Inc. DTC-1 fuel rack controller. The DTC-1 fuel rack control unit operated a small servo motor that was connected via a stainless steel rod and servo-saver spring unit the engine fuel rack, which can be seen in Figure 22.

**Figure 22: Servo motor and fuel rack control linkages.**

Fuel rack set points were entered manually on the DTC-1 or from a computer through a serial connection to the system. See the following Figure 23 for an image of the system control rack containing the DTC-1 fuel rack controller. Details illustrating all connection points in the rear of the DTC-1 given in Figure A-7.


**Figure 23: DTC-1 used for SETC fuel rack control.**

### *3.9.3 Invertek Optidrive Plus*

The dynamometer motor was controlled directly by the Invertek Opti-drive Plus (ODP) which was mounted on the wall beside the engine-dyno skid and shown below in Figure 24. The Invertek was capable of controlling motors of up to 150 hp and absorbing up to 20 hp of electrical energy from the motor before dumping to an external resistor bank, in this case the previously mentioned Chromalox immersion heater.

**Figure 24: Invertek Optidrive Plus.**

### *3.9.4 Smarty Drive Control*

A Bardac Smarty controller device that could communicate directly with the Invertek, as well as make use of the Lebow in-line torque measurement device was used for system control. A picture of this control system with Bardac Smarty controller can be found below in Figure 25.

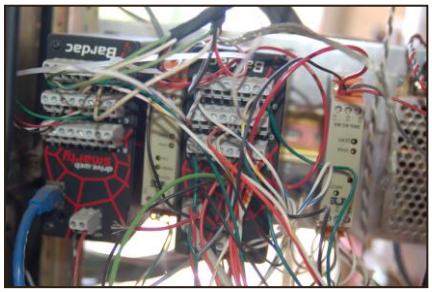

**Figure 25: Bardac Smarty dynamometer control setup.**

## 3.10 Safety

During the development of the laboratory test cell, many safety measures were taken into account. An emergency shut off button was used to remove power from the system, as well as closing a fuel shutoff solenoid on the engine. A tubing air line system is also in place located above all rotating parts between the engine and dynamometer. If a rotating part failed and broke the air line, a pressure sensor would shut off fuel to the engine.

## 3.11 SETC Dynamometer Calibration

### *3.11.1 Lebow Torque Cell Calibration*

It was necessary to calibrate the Lebow torque transducer to be sure that the measured torque values corresponded to the real torque values. To perform this task a torque arm shown Figure 26 was fabricated, detailed, and weighed. Calibrated weights were hung from the torque arm using a calibrated 1 pound basket. The torque readings from the moment created by each weight as it was added to the total stack was compared to calculated values of what the actual torque should be. The zero and span of the strain gauge amplifier were altered, as well as the torque value offset within the Smarty unit to calibrate the system to read proper torque values.

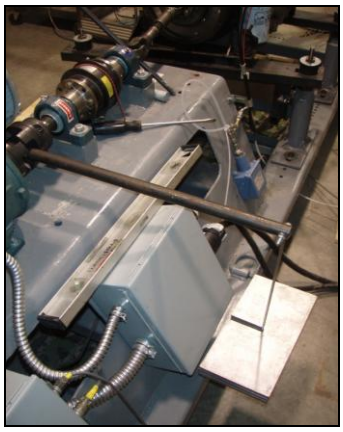

**Figure 26: Lebow torque cell calibration setup.**

Once these parameters were set, torque readings from the Lebow were within 1% of actual calculated value. Figure 27 below gives a graphical representation of the linear curve associated with the measured torque values compared to the calculated torque values after calibration of the Lebow.

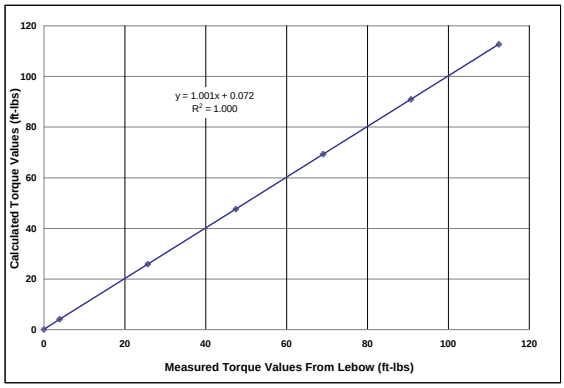


**Figure 27: Measured torque readings from Lebow torque cell after torque cell calibration compared with manually calculated torque values.**

### *3.11.2 ODP and Lebow Torque Output Comparison*

With the inline Lebow torque transducer in operation, a comparison was made between the inferred torque readings of the ODP and the actual measured torque values received from the Lebow. By this time it had become apparent that even at a zero set torque, there was still about 5 ft-lbs of residual torque being produced by the internal current of the motor. The goal of this

comparison was to determine if there was a linear equation that could be applied to the ODP to accurately produce a desired torque value. ODP and Lebow output torque values compared to input torque setpoints are shown in Figure 28.

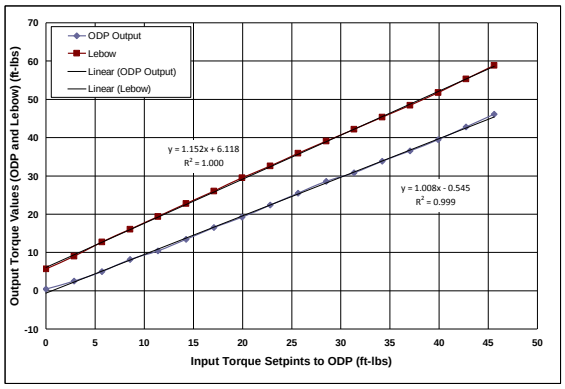


**Figure 28: Output torque values from both the ODP and Lebow as compared to input torque set points.**

As can be seen in Figure 28, there was an obvious discrepancy between the ODP inferred torque and the torque measured by the inline Lebow torque transducer. It was necessary to setup the software with a built-in calibration equation that supplied a corrected input value to the ODP in order to achieve a requested actual torque load value to the motor. A comparison between input torque values and measured output values is shown below in Figure 29. Equation 3 was used to calibrate the ODP and Lebow torque input values.

$$\tau_{Input} = 152.25(\tau_{Desired}) - 930.51 \qquad \text{Equation 3}$$

In which,

$\tau_{Desired}$ = the desired output torque value in (ft-lbs) (N-m)

$\tau_{Input}$ = the determined input value to the ODP in (ft-lbs) (N-m)

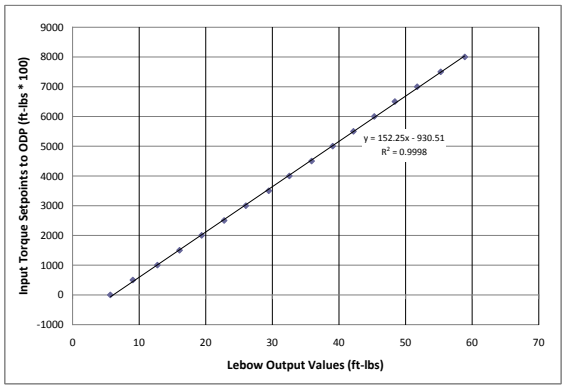


**Figure 29: Input torque setpoints as compared to Lebow output torque values.**

### *3.11.3 Dilution Tunnel Blower Setup and Commissioning*

The SETC dilution tunnel blower was controlled by an Invertek ODP unit similar to the one used to control the dynamometer rated for 10 horsepower motors. Communication with the ODP drive was performed through a Bardac Smarty via an Ethernet connection with a PC. Operation of the blower proved to be successful as speed was input at the PC/Smarty interface produced the appropriate response from the blower. A more complete description of calibrating the CVS system is described in Section 4.3.3.

# Chapter 4: Experimental Setup and Procedure

# 4 Experimental Setup and Procedures

## 4.1 Introduction

The following section describes the process and equipment used during experimental commissioning of the SETC. All data collection and equipment was predominantly setup to follow CFR Title 40, Part 1065 [45]. There was some departure from 1065 during the initial testing. These exceptions are noted as necessary.

## 4.2 Test Engine

A used twenty-seven horsepower four cylinder Isuzu diesel engine with an estimated 5,000 running hours was acquired to operate for commissioning of the SETC. This engine was donated to CAFEE by Belt Transfer, Inc. located in Ravenswood, WV and was removed from a Thermo King TRU which had been sitting unused for some time. Figure 30 shows the engine in its initial condition after pick up from Belt Transfer, Inc.

**Figure 30: Thermo King four cylinder 27 horsepower diesel engine.**

The engine was mounted to the test stand and connected to the dynamometer via a drive shaft and a Vulcan torsional damper. The Vulcan rubber coupling was an existing component

from the EERL, and the flange for mounting the coupling to the engine flywheel was designed by Balaji Seward of CAFEE, and manufactured by Wilson Works, Inc

Due to the visibly rough condition of the engine, and the obvious length of time that it had been sitting, there was some initial concern that the engine would have trouble running properly. This concern was eliminated however, as after some careful wiring of an ignition system, an oil change, and bleeding of the fuel lines; the engine was able to run without incident.

## 4.3 Test Cell Data Acquisition System

### *4.3.1 Analytical Trailer Mobile Emissions System and Dilution Tunnel*

SETC commissioning was performed with CAFEE's existing mobile emissions testing laboratory, as seen in Figure 31, be used. This equipment contains a complete emissions test bench of gaseous emissions analyzers and a self contained dilution tunnel system.

**Figure 31: CAFEE Transportable Analytical Trailer Emissions Laboratory.**

### *4.3.2 Data Collection and Communications System*

For commissioning of the SETC, a data collection system was setup based around one main PC operating a Microsoft Visual Basic 6 program to control the lab functions, read and send data from the Smarty drive units. The software also read data from a National Instruments

SCC data acquisition block, and communicated via serial port with the Dyne Systems DTC-1, fuel scale, and emissions bench computer system within the analytical trailer.

The SETC control software was developed over several months with vast contributions from CAFEE's Richard Atkinson. The program was capable of controlling engine fuel rack, dynamometer torque set points, performing an engine map, and reading and operating a steady state test cycle. An image of the main control system PC running the SETC control software can be seen in Figure 32.

**Figure 32: Small Engine Test Cell commissioning main control PC.**

### *4.3.3 Subsonic Venturi Dilution Tunnel Flow Meter and CVS Calibration*

For this testing the laboratory operated at a lower flow rate and the smaller 3.65" throat venturi was used to measure dilution tunnel flow. In order to calibrate the venturi, a laminar flow element (LFE) was mounted in series with the venturi and the measured flow through the venturi was compared to that measured from the LFE. The LFE unit was calibrated to have a known pressure drop of 8 inches of $H_2O$ at 1,000 scfm, and was complete with documentation describing the equations and constants necessary to calculate flow based on gathered absolute pressure, differential pressure across the LFE, and intake temperature. The calibration setup is shown below in Figure 33.

**Figure 33: Venturi flow meter calibration setup.**

The Bardac Smarty drive unit was programmed to run the blower and perform the necessary operations to operate the blower during the calibration as well as during future dilute testing with this tunnel section. Based on the given theoretical performance curve documentation of the venturi from Flow-Dyne Engineering, Inc., it was known that the flow through the venturi would be calculated based on Equation 4 [46].

$$Q_{Venturi} = f\left[\sqrt{\frac{\Delta P}{P_1}}\right] * \left[\frac{P_1}{\sqrt{T_1}}\right] \qquad \text{Equation 4}$$

Equation 4 simplifies to,

$$Q_{Venturi} = f\left[\sqrt{\frac{\Delta P * P_1}{T_1}}\right] \qquad \text{Equation 5}$$

in which,

$Q_{Venturi}$ = the flow through the venturi in ($ft^3$/min) ($m^3$/s)

$\boldsymbol{\Delta P}$ = differential pressure in inches of $H_2O$

$\boldsymbol{P_1}$ = absolute pressure at the intake of the unit in (psi) (kPa)

$\boldsymbol{T_1}$ = the intake temperature in percent of 400 K as read from the RTD (%)

For the purposes of this paragraph, the parameters within the brackets of Equation 5 will be referred to as the "venturi function." For calibration, drive points for the blower were set with the Smarty based on 100% of full blower drive, and for each drive point the parameters of absolute pressure, differential pressure, and intake temperature were measured for both the LFE and venturi. LFE flow was calculated based on air viscosity, μ in micro poise, actual flow with given conditions, and then flow corrected for standard conditions of 70º F, and 14.7 psi as barometric pressure all using Equation 6 and Equation 7.

$$\mu_{calc} = \frac{(14.58 * (273.15 + T_1)^{1.5})}{(110.4 + (273.15 + T_1))} \qquad \text{Equation 6}$$

$$Q_{Actual} = ((B * \Delta P) + C(\Delta P)^2)\left[\frac{181.87}{\mu_{calc}}\right] \qquad \text{Equation 7}$$

Where,

$T_1$ = the venturi intake air temperature in (K) (°F)

$Q_{Actual}$ = the actual flow through the LFE in ($ft^3$/min) ($m^3$/s)

***B*** = LFE calibration constant provided by Meriam of 0.00126

***C*** = LFE calibration constant provided by Meriam of -0.248

Flow is then corrected for standard conditions using Equation 8.

$$Q_{Std} = Q_{Actual}\left[\frac{P_1}{14.696\,psi}\right] \times \left[\frac{294.261K}{(T_1 + 273.15)K}\right] \qquad \text{Equation 8}$$

Where,

$Q_{Std.}$ = the air flow corrected for standard temperature and pressure in ($ft^3$/min) ($m^3$/s)

The values for the venturi function calculated from temperature and pressures across the venturi at each blower drive percentage were then plotted against calculated values for flow rate through the LFE in order to obtain a linear relationship in the form of Equation 9.

$$Q_{Venturi} = k\left[\sqrt{\frac{\Delta P * P_1}{T_1}}\right] + b \qquad \text{Equation 9}$$

Where

***k*** = a linear equation multiplying constant

***b*** = a linear equation calibration offset

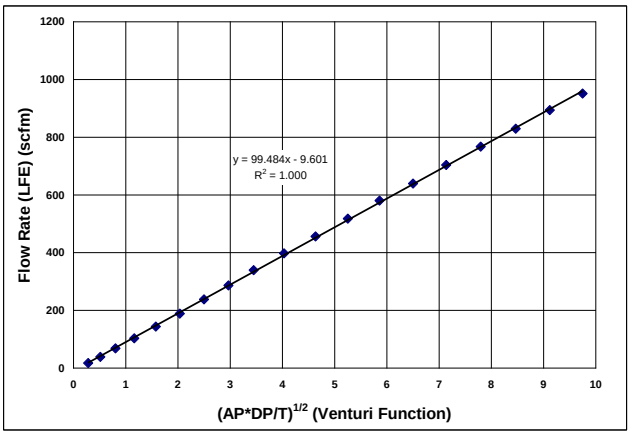


**Figure 34: Plot of Venturi Function vs. LFE flow rate to determine a linear relationship.**

From the trend line associated with the graph in Figure 34, flow rate through the venturi was then calculated using Equation 10.

$$Q_{Venturi} = 99.48 \times \left[\sqrt{\frac{\Delta P \times P_1}{T_1}}\right] - 9.6 \qquad \text{Equation 10}$$

The missing values of *k* and *b* from Equation 4 have now been found to be 99.48 and -9.6 respectively. This equation was then entered into the Smarty programming to control blower

flow rate during testing. The resulting correlation between input flow rate and measured flow between the venturi and LFE is described in Figure 35.

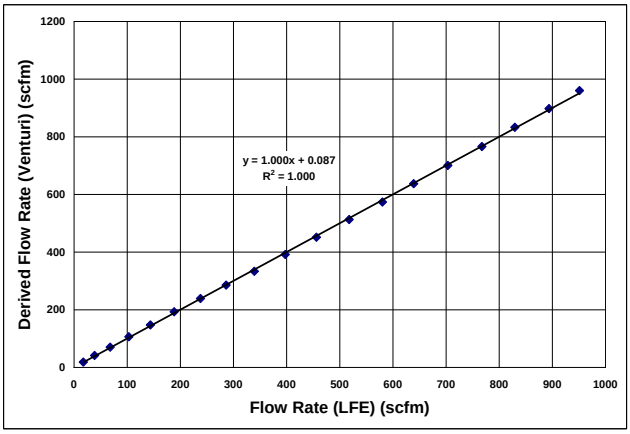


**Figure 35: Comparison of flow rate measured across the LFE and venturi flow meters.**

### *4.3.4 Particulate Matter Sampling System*

As the analytical trailer uses a Part 86 compliant particulate matter (PM) sampling system, it was necessary to install a separate gravimetric PM sampling system designed for use under the CFR 1065 regulations. An external PM box, shown in Figure 36 was removed from the EERL was completed, and installed outside of trailer.

It is important to note that in using the Mobile Analytical Trailer, there was no secondary dilution air system as part of the PM sampling package. During emissions testing, the secondary dilution air system helps to maintain filter face temperatures at the required 117 °F, as well as maintain a minimum dilution ratio of between 5:1 and 7:1 through the PM sampling system [45]. It was possible to build a secondary dilution system to be retrofitted to the Analytical Trailer, however due to time and funding constraints, the measure was omitted from the system. The results of the effect the lack of secondary dilution air had on the PM collection system are discussed again in Section 5.4.7.

**Figure 36: CFR 1065 compliant 1065 sampling system.**

### *4.3.5 Gaseous Emission Sampling System*

Gaseous emissions were sampled and recorded using probes mounted within the dilution tunnel which were connected to the trailer's internal analyzer bench and data acquisition system. This bench consisted of analyzers, shown in Figure 37, for hydrocarbon, oxides of nitrogen, carbon monoxide, and carbon dioxide.

**Figure 37: Mobile analytical trailer emissions sampling bench.**

### *4.3.6 Exhaust Gas Analyzers*

Oxides of nitrogen ($NO_x$) were measured using two, a CAI 400 HCLD, and CAI 600 series NO/NOx analyzers. Both of these units operate using the chemiluminescent reaction between ozone ($O_3$) and nitric oxide (NO), which produces nitrogen dioxide ($NO_2$) and oxygen

($O_2$). The intensity of the light produced during this reaction is proportional to the mass flow rate of $NO_2$ into the analyzer's reaction chamber. During the commissioning of the SETC, these analyzers were operated in $NO_x$ mode, in which, the sample was routed through an internal $NO_2$ to NO converter, and the resultant reaction was directly proportional to the total concentration of $NO_x$.

Exhaust gas hydrocarbons (HC) were measured with a Rosemont 402 HC analyzer. Passing the sample through a hydrogen/helium flame within the analyzer produced ions which were collected on internal electrodes. Absorption of these ions by the electrodes produces a current within the internal circuitry of the analyzer which is measured and related to the amount of carbon atoms within the exhaust sample [47]. Prior to testing, the internal sample pump within the Rosemont failed and was replaced.

Horiba A1A-210LE and A1A-210 analyzers were used to measure low and high level carbon monoxide emissions during testing. Carbon dioxide ($CO_2$) was measured with a Horiba AIA-210. These CO/$CO_2$ analyzers operated with a Non Dispersive Infrared (NDIR) system, which utilized infrared light absorption of the sample gas. The sample gas passing through the sensor absorbed a certain wavelength within the infrared spectrum and allowed the remaining wavelengths to pass through. The analyzer measured the amount of absorbent gas by detecting the amount of infrared energy allowed to pass through the sample gas [48].

### *4.3.7 Background Bag*

During each test, background gas was sampled and collected into an 80-liter Tedlar background bag. This task ensured that any levels of the analyzed pollutants that existed in the background air during testing were accounted for during total emission calculations. This sample

was directed through the analyzers at the end of each test, and recorded along with the full test emissions data.

### *4.3.8 Engine Intake Air Measurement*

Engine intake air flow was measured using a Meriam Technologies laminar flow element (LFE) mounted inline of the engine's intake piping. This LFE contained a honeycomb structure of small capillary tubes. These capillary tubes converted any turbulent air entering the intake piping into a laminar flow and in doing so a pressure drop was produced. Measuring this pressure drop, along with the use of calibration coefficients and data provided by Meriam, allowed for calculation of intake air flow. For this calculation, Equation 11 was used.

$$Q_{Actual} = ((B * \Delta P) + (C * \Delta P^2))\left[\frac{\mu_{Standard}}{\mu_{Flow}}\right] \qquad \text{Equation 11}$$

Where,

$Q_{Actual}$ = Volume flow rate of air through the LFE in ($ft^3$/min) ($m^3$/s)

$\boldsymbol{\Delta P}$ = The pressure drop through the LFE across the capillary tubes in inches of $H_2O$

$\boldsymbol{B}$ = Meriam Instruments LFE calibration constant of $1.27637*10^1$

$\boldsymbol{C}$ = Meriam Instruments LFE calibration constant $-5.8276*10^{-2}$

$\boldsymbol{\mu_{Standard}}$ = The kinematic viscosity of air at standard temperature and pressure in (micro poise) (lb-sec/$ft^2$) (kg-s/$m^2$)

$\boldsymbol{\mu_{Flow}}$ = The corrected kinematic viscosity of the actual flow in (micro poise) (lb-sec/$ft^2$) (kg-s/$m^2$)

Flow viscosity was calculated and corrected for viscosity variations with Equation 12.

$$\mu_{Flow} = \frac{14.58 * (T_I + 273.15)^{1.5}}{110.4 + (T_I + 273.15)} \qquad \text{Equation 12}$$

Where,

$T_1$ = The engine intake air temperature (K)

And finally the intake air flow calculation was corrected for standard temperature and pressure with Equation 13,

$$Q_{Standard} = Q_{Actual}\left[\frac{P_{Abs}}{14.69595}\right]\left[\frac{294.21111}{273.15 + T_I}\right] \qquad \text{Equation 13}$$

Where,

$Q_{Standard}$ = Volume flow rate of air through the LFE corrected for standard conditions in ($ft^3$/min) ($m^3$/s)

$P_{Abs}$ = The absolute pressure at the intake of the LFE

The Meriam LFE used during testing was a model number 50MC2-2 with a 2 in. I.D. Differential pressure was across the capillary tubes was measured with an Ashcroft differential pressure transmitter mode IXLdp with a range of 10 inches of water, and an output voltage range of 1 to 5 volts. Intake temperature was measured with a J-Type thermocouple.

## 4.4 Engine Mapping Procedure

A map of an internal combustion engine is a measurement of the maximum torque throughout the speed range of the engine tested. For the small engine test cell commissioning the engine map was then used to determine an emissions test cycle. The map was performed on the test engine in accordance with the regulations outlined in CFR 1065.510 [45]. This mapping

procedure and controlled by the SETC control software and performed using a continuous sweep of increasing engine speed at full load throughout the engine's speed range beginning at idle with full load and increasing engine speed 8 rpm/second through the full speed range. Results of the map show a maximum horsepower of 26.7 hp at 2480 rpm, and a maximum torque of 61.1 ft-lbs at 1850 rpm. The resulting map is shown in Figure 38.

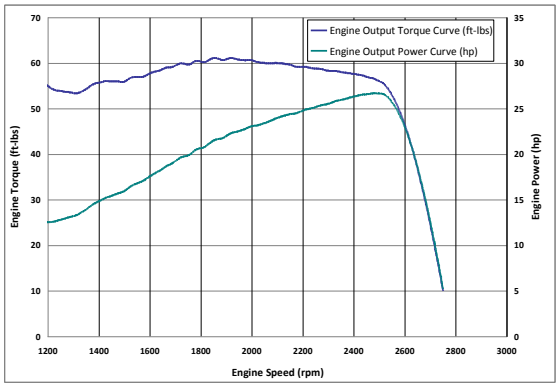


**Figure 38: Engine power and torque curves resulting from engine map.**

## 4.5 Test Cycles

### *4.5.1 Steady State Test*

For commissioning of the lab, a steady state cycle was used in the form of an 8 mode ISO-8178 C1 cycle for off-road engines in compliance with CFR 1065.512 [45]. The normalized ISO-8178 test cycle was as described in Table 3 [49]. Applying the normalized test cycle to the engine map results, the subsequent finalized test cycle for commissioning of the test cell was as described in Table 4.

**Table 3: Normalized IS0-8178 C1 test cycle [49].**

| Mode | 1 | 2 | 3 | 4 | 5 | 6 | 7 | 8 |
|---|---|---|---|---|---|---|---|---|
| Speed | Rated Speed | | | | Intermediate Speed | | | Idle |
| Torque (%) | 100 | 75 | 50 | 10 | 100 | 75 | 50 | 0 |
| Weighting Factor | 0.15 | 0.15 | 0.15 | 0.1 | 0.1 | 0.1 | 0.1 | 0.15 |

**Table 4: Final steady state test cycle.**

| Mode | 1 | 2 | 3 | 4 | 5 | 6 | 7 | 8 |
|---|---|---|---|---|---|---|---|---|
| Speed (rpm) | 2200 | 2200 | 2200 | 2200 | 1500 | 1500 | 1500 | Idle |
| Torque (ft-lbs) | 60 | 46 | 31 | 6 | 60 | 46 | 31 | 0 |
| Total Sample Time (sec) | 200 | 200 | 200 | 200 | 200 | 200 | 200 | 240 |
| PM Sample Time (sec) | 150 | 150 | 150 | 100 | 100 | 100 | 100 | 150 |

### *4.5.2 Test Plan and Total Tests Performed*

A test plan was developed for the commissioning tests for the SETC. Six steady state tests, named and ordered A through F, were run following the steady state test cycle shown in Table 4, and data for PM, $CO_2$, CO, $NO_x$, and HC were collected. Three of the six tests were run as a baseline without aftertreatment, and three were run with a generic passive regeneration diesel particulate filter (DPF) with an internal catalyst layer. As mentioned in Section 2.9.2 this DPF acted as a particulate trap collection PM produced by the engine. The DPF was also equipped with an internal catalyst layer to reduce the exhaust constituents of HC and CO along with PM. It must be noted that, although the test plan called for six tests, the data from seven steady state tests were kept for comparison. The second test, Test B, lacked PM data, however all gaseous emissions data were still applicable for commissioning comparison.

### *4.5.3 Transient Testing*

A transient cycle routine was developed as part of the SETC control software that followed the EPA Non Road Transient Test Cycle [50]. Several attempts to operate this routine were made, however with the current mechanical fuel rack linkage; the fuel rack control was not adequate to follow the transient target speeds. It does appear that the dynamometer and control scheme would be able to handle this type of testing procedure given that an engine with a more accurate fuel rack control method were to be used. Results of transient attempts will be described

further in the Section 5.3 of this document. Figure 39 shows the normalized EPA Non Road Transient Cycle [50].

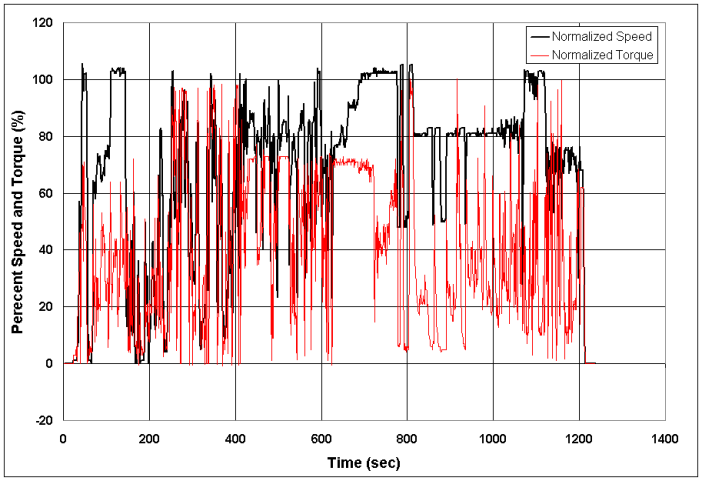


**Figure 39: Normalized EPA Non Road Transient Cycle.**

# Chapter 5: Experimental Testing Analysis and Emissions Results

# 5 Experimental Testing Analysis and Steady State Emissions Results

## 5.1 Introduction

The following section compares the results of seven steady state SETC commissioning tests, as well as details concerning the attempt at performing a transient test. As previously mentioned the steady state test plan called for only six tests, however during Test B, no PM filter was placed within the PM sampling system, and thus there is no PM data for Test B. The remaining gaseous emissions data pertaining to Test B were still valid for comparison. Table 5 lists all steady state tests performed during test cell commissioning. Carbon balance data for validation of emissions results is given in Section 5.4.5.

**Table 5: Performed steady state tests.**

| Test Name | Aftertreatment | Notes |
|---|---|---|
| A | None | Dyno fault, end of mode 1 |
| B | None | No PM Data |
| C | None | |
| D | None | |
| E | DPF | |
| F | DPF | |
| G | DPF | |

## 5.2 Steady State Testing and Test Cycle Validation

### *5.2.1 Average Speed and Torque for All Tests*

Referring to Section 4.5.1, each test had specific speed and torque set points to follow. Figure 40 gives a graphical representation of the average speed outputs of all tests when compared to the speed input values. The blue line shows the average speed outputs for all tests during cycle sample time, and the red line represents the set point speed throughout the test. As one can see, on average, when the ODP is given a certain speed input, the speed of the engine can be held as constant. One discrepancy can be seen in the plot, where during Test A, an error occurred within the ODP causing a loss of load to the motor. This error occurred so late in mode

1 of Test A, that the test was continued, and restarted in mode 2. With the loss of dyno load for this instant, engine speed increased upsetting the average at that stage in the plot. This error and corrective measures are discussed further later within this document. The lowest average speeds shown in the plot are for the idle mode. This mode had no real speed set point, as the dynamometer was simply turned off, and the fuel rack set to zero to allow the engine to settle to its idle speed.

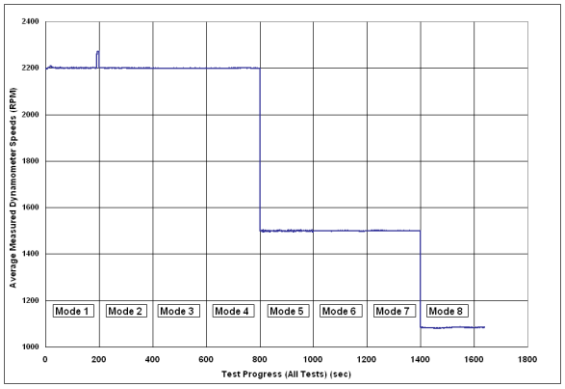


**Figure 40: Average speed outputs for all tests compared to the speed set points.**

In the same manner that the dynamometer and control system were able to respond appropriately to a specified speed input, the system was found to also handle torque input values as well. The average output torque values for all seven tests as compared to the torque input set points throughout the progress of the tests are shown in Figure 41. It is evident that on average, the torque outputs match that of the set point torque values. Modes 1 and 5 (from 0 to 200 and from 800 to 1000 seconds respectively) show some discrepancy, and this will be detailed further in Section 5.2.2. The remaining modes show an almost exact match in output and set point torques, and the final idle mode shows a torque reading slightly below zero. For the idle mode, the dynamometer was turned off to eliminate the residual torque even with an ODP set point of zero. The slightly negative torque reading can be attributed to the Lebow reading itself, as well as some friction within the dynamometer motor bearings. Despite being properly zeroed, the

Lebow seemed to show some misleading values towards to very low end of the range. A reminder the Lebow had a range of 20,000 in-lbs, equating to approximately 1600 ft-lbs. It is reasonable to see how at very low torques, there would be some error in the reading with a device of such a large range attempting to measure such low torques. Further calibration of the torque sensor towards the lowest end of its range could possibly have helped with lower torque measurements.

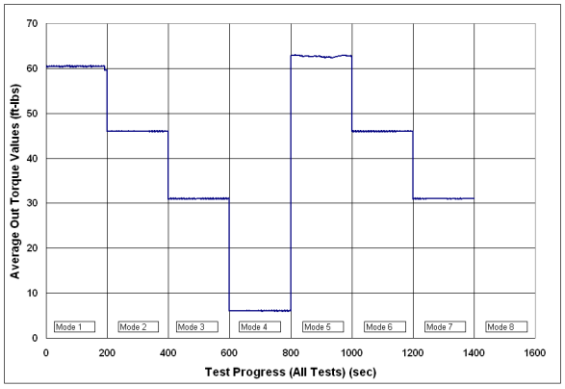


**Figure 41: Average torque output readings during test progress as compared to input torque values.**

### *5.2.2 Specifics for Modes 1 and 5*

The control scheme operating mode 5 differs from the remaining modes. Mode 5 runs at maximum torque, and intermediate speed, 1500 rpm. During initial test attempts this mode operated the same as all others, the fuel rack would settle to the input speed, and the dynamometer would load the engine to the specified torque. However, with mode 5, all attempts to smooth out this process within the software failed, and each time the test would make it to mode 5, the fuel rack would settle at 1500 rpm, and the dynamometer would begin to load the engine. As load increased the fuel rack would increase to maintain speed, and would typically find itself in the proper position of 60 ft-lbs and 1500 rpm, but during the stabilization of the

mode, each time the load on the engine would become too much, and bring the engine speed down enough to completely stall the engine. The software was modified so that during mode 5, the software would hand over full control to the smarty alone which would apply the maximum torque necessary to hold the engine at 1500 rpm. The switch was triggered by a torque set point value of 70 ft-lbs. This "trigger set point" was chosen generically, and entered into the test cycle data file. Though this method was only a "work around" for the Isuzu CP-201 used for these particular tests, it proved to work quite well in managing the set points of mode 5. The "work around" may not be required for other engines operating in the SETC. Measured speed and torque values for all tests during mode 5 are shown in Figure 42 and Figure 43.

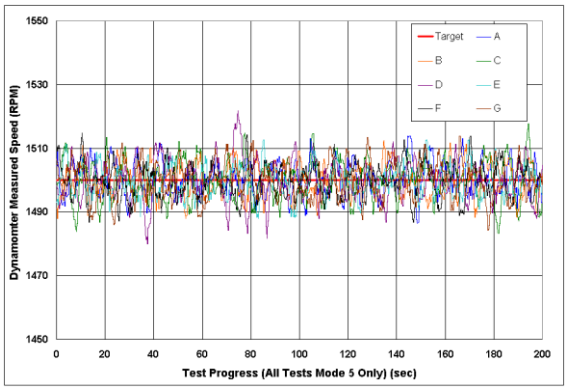


**Figure 42: Measured speed values during mode 5 for all tests.**

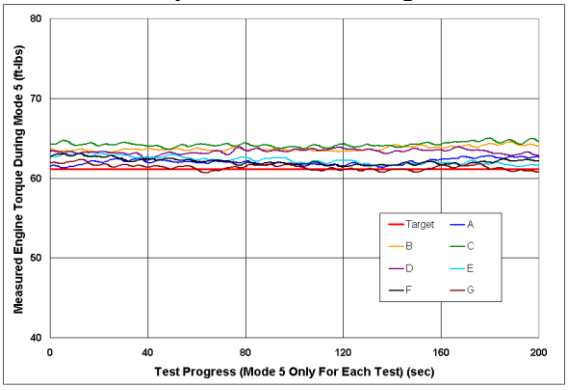


**Figure 43: Measured torque values for all tests during mode 5.**

It should also be mentioned that this same method was also applied to mode 1 for some time. It was decided that since mode 1 was to be at maximum torque as well, handing over control to the Smarty would work for mode 1 as well. However, during mode 1, operating with the Smarty only at 2200 rpm was found to produce torque values of up to 66 ft-lbs. Torques of this magnitude did not appear when the engine map was performed, and was also observed to cause an issue with the dynamometer itself. Torque values this high uncovered the high end envelope of the dynamometer, and caused an error within the motor and ODP dynamometer system overloading the motor and causing a fault in the ODP known as "IT TRIP" or an over current fault. This can be seen in Test A, during which at the end of mode 1 the motor faulted and released all load from the engine allowing the engine speed to spike. Once more, as this affected only several seconds towards the end of mode 1, the test was restarted and continued in mode 2. To prevent this from occurring, mode 1 was restored to operate under the control of the developed SETC control software with a maximum torque set point of 60 ft-lbs. This error never occurred during mode 5, as when operating with the Smarty applying maximum torque at 1500 rpm, the highest torque values obtained were oscillating between 62 and 64 ft-lbs, which seemed to be just below the overload for the dynamometer system.

### *5.2.3 Quantifying Deviation from the Reference Test Cycle*

CFR Section 1065.514 specifies that all measured speed values must remain within a tolerance of 2% of the reference value, and that measured mean speed and torque values must be within 1% of the reference [45]. All cycle validation calculations were performed using the test data, which was collected at 10 Hz. Figure 44 displays the percent difference from the reference speed at each point for each test over the entirety of the test periods. The idle mode has been

removed from this graph as there was no particular set point other than completely removing any load on the engine and setting fuel rack to zero.

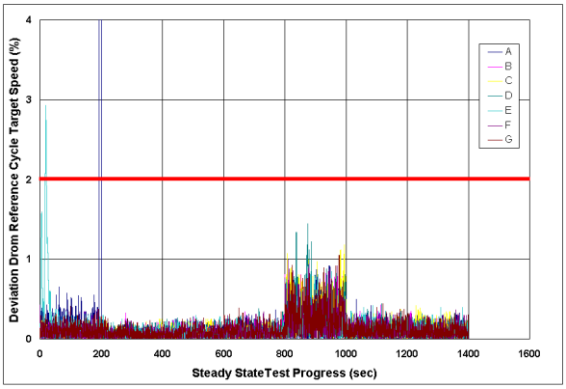


**Figure 44: Calculated % differences of speed outputs from reference speeds for all tests.**

As shown in Figure 44, the percent difference of the measured speeds from that of the set points fall within the required 2% to be compliant with CFR 1065 cycle validation [45]. The only discrepancy to speak of stems from the ODP and dynamometer over current drop out that occurred during Test A, which was subsequently resolved. There are some higher values that seemed to occur during mode 1 of Test E, which are most likely the result of the lab beginning to take data prior to full mode stabilization. Mode 5 shows some higher difference values than all other modes as it is controlled only by the Smarty drive and not the SETC control software. The increased noise level of the speed feedback during mode 5 still falls within the 2% tolerance requirement. This same idea was applied to measured torque values during testing as well. Results from the comparison of measured and reference torque values can be seen in Figure 45. Once more, the idle mode at the end of each test has been omitted. Additionally, mode 5 for each test has not been shown in Figure 45. Given the difference in control operation during mode 5, the measured torque value is not compared to an input set point from the test cycle file.

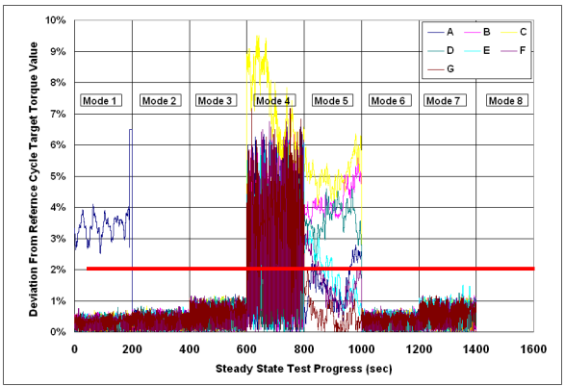


**Figure 45: Deviation from target torque values for each test over the full test cycle.**

Instead, torque values during mode 5 were compared to the measured maximum mapped engine torque. This was also the case for mode 1 of Test, A, which can also be seen in Figure 45 and was later changed for all subsequent tests after resulting in drop out of the ODP unit. Obviously, there was some issue within mode 4, between 600 and 800 seconds of test progression. It is at these points where one can see the difficulties that the dynamometer had in attempting to maintain low torque loads. With deviations up to 9.5% from the reference value, torque values as low as the target value of 6 ft-lb, such as the case during mode 4 of the test cycle, are noticeably difficult for the dynamometer to hold. Again, this is a result of the residual torque properties of the motor itself. While trying to hold 6 ft-lbs, the ODP applies very little increase to the torque load of the motor, which causes the variation in output values. With the exception of mode 4, all remaining modes fall within the required minimum of 2% deviation from the reference torque value.

Obviously, the issue with mode 4 was a problem, as data during mode 4 was technically not quality data since the test cycle was not valid at those points. The issue also repeats itself during mode 5 as often times the measured torque value differs from the mapped engine torque by more than 2%. With further refinement of the lab control software, it seems possible that these issues could be resolved. As mentioned before, the problems that occurred with mode 5

were specific to this engine, and are not representative of what would necessarily occur with a different engine. The issues with mode 4 however, were more specific to the dynamometer and its ability to hold low torque loads consistently. This could be resolved with more modification to the internal parameters of the ODP controller. Bardac does not allow the user direct modification of the ODP's internal PID, so working closely with those at Bardac to improve upon the PID to handle low and fine loads could lead to a resolution. Table 6 gives a summary of the compliance of mean measured speeds for all tests with the 1% deviation requirement. Numbers highlighted in green represent percent differences from the reference set point that met the 1% requirement.

**Table 6: Comparison of measured average speeds to reference.**

| | Mode | 1 | 2 | 3 | 4 | 5 | 6 | 7 |
|---|---|---|---|---|---|---|---|---|
| Test | Speed Set Point (RPM) | 2200 | 2200 | 2200 | 2200 | 1500 | 1500 | 1500 |
| A | Measured Average (RPM) | 2219.68 | 2199.93 | 2198.66 | 2199.06 | 1500.31 | 1499.92 | 1500.26 |
| | % Difference | 0.89 | 0.00 | 0.06 | 0.04 | 0.02 | 0.01 | 0.02 |
| B | Measured Average (RPM) | 2200.44 | 2199.57 | 2199.04 | 2199.31 | 1500.42 | 1499.06 | 1499.79 |
| | % Difference | 0.02 | 0.02 | 0.04 | 0.03 | 0.03 | 0.06 | 0.01 |
| C | Measured Average (RPM) | 2200.45 | 2199.64 | 2198.45 | 2200.71 | 1500.59 | 1500.36 | 1500.92 |
| | % Difference | 0.02 | 0.02 | 0.07 | 0.03 | 0.04 | 0.02 | 0.06 |
| D | Measured Average (RPM) | 2200.19 | 2199.52 | 2198.51 | 2198.79 | 1500.32 | 1499.73 | 1499.88 |
| | % Difference | 0.01 | 0.02 | 0.07 | 0.05 | 0.02 | 0.02 | 0.01 |
| E | Measured Average (RPM) | 2203.51 | 2199.67 | 2198.16 | 2199.46 | 1500.09 | 1499.17 | 1499.41 |
| | % Difference | 0.16 | 0.02 | 0.08 | 0.02 | 0.01 | 0.06 | 0.04 |
| F | Measured Average (RPM) | 2200.71 | 2200.70 | 2199.17 | 2199.52 | 1500.22 | 1499.93 | 1501.11 |
| | % Difference | 0.03 | 0.03 | 0.04 | 0.02 | 0.01 | 0.00 | 0.07 |
| G | Measured Average (RPM) | 2200.63 | 2200.87 | 2198.90 | 2199.50 | 1500.11 | 1499.49 | 1500.43 |
| | % Difference | 0.03 | 0.04 | 0.05 | 0.02 | 0.01 | 0.03 | 0.03 |

Again, the same 1% for the mean measure value applies for the engine torque throughout the tests, and Table 7 shows how the tests performed with regards to torque set points. The issues with mode 5 persist even with the mean comparison. It must be noted here, that as mode 5 had no actual set point torque, the measured mean values were compared to the maximum mapped engine torque of 61 ft-lbs. The CFR 1065 requirements for cycle validation state that for EPA the tests must meet the requirements unless it can be determined that failing to meet the specification is related to engine performance and not shortcomings of the dynamometer or laboratory equipment [45]. The complications of mode 5 are certainly inherent to engine performance rather than equipment capabilities. The remaining modes show good agreement with the reference

torque set point. The previously mentioned problems with mode 1 of Test A arise once more here and remain outside of the validation criteria, and mode 6 of Test C misses the 1% requirement as well. The complications mode 6 can most likely be attributed to lack of low end resolution with the torque sensor. To reiterate, the Lebow torque transducer used in commissioning of the SETC had a range of 0 to 1600 ft-lbs. As this application dealt with loads at and below 65 ft-lbs, the range of the torque transducer was unnecessarily high. However, the sensor used was one that already belonged to the CAFEE group and saved the group from needing to purchase a new device. Mode 6 of Test C is the only measured mean torque that truly does not meet the cycle validation criteria, as it is due to an issue inherent to the Lebow torque sensor range. Installing a more appropriately ranged torque sensor for future small engine tests would alleviate this problem.

**Table 7: Comparison of measured average torque values to the reference.**

| | Mode | 1 | 2 | 3 | 4 | 5* | 6 | 7 |
|---|---|---|---|---|---|---|---|---|
| Test | Speed Set Point (RPM) | 60 | 46 | 31 | 6 | 61 | 46 | 31 |
| A | Measured Average (RPM) | 62.99 | 46.00 | 31.00 | 6.00 | 62.01 | 46.01 | 31.00 |
| | % Difference | 4.98 | 0.00 | 0.00 | 0.00 | 1.65 | 0.02 | 0.01 |
| B | Measured Average (RPM) | 60.00 | 46.01 | 31.01 | 6.03 | 63.65 | 46.02 | 31.02 |
| | % Difference | 0.00 | 0.02 | 0.04 | 0.52 | 4.35 | 0.04 | 0.06 |
| C | Measured Average (RPM) | 59.99 | 46.00 | 31.01 | 6.44 | 64.17 | 46.01 | 31.00 |
| | % Difference | 0.02 | 0.01 | 0.02 | 7.34 | 5.20 | 0.02 | 0.01 |
| D | Measured Average (RPM) | 60.00 | 46.01 | 31.01 | 6.01 | 63.28 | 46.00 | 31.01 |
| | % Difference | 0.00 | 0.01 | 0.03 | 0.20 | 3.74 | 0.01 | 0.02 |
| E | Measured Average (RPM) | 59.99 | 46.01 | 31.01 | 6.02 | 62.19 | 46.01 | 31.01 |
| | % Difference | 0.02 | 0.02 | 0.02 | 0.27 | 1.96 | 0.02 | 0.04 |
| F | Measured Average (RPM) | 59.99 | 46.01 | 31.01 | 6.01 | 62.04 | 46.01 | 31.02 |
| | % Difference | 0.01 | 0.03 | 0.03 | 0.18 | 1.70 | 0.02 | 0.07 |
| G | Measured Average (RPM) | 60.00 | 46.00 | 31.01 | 6.01 | 61.30 | 46.01 | 31.01 |
| | % Difference | 0.00 | 0.00 | 0.02 | 0.19 | 0.50 | 0.01 | 0.03 |

## 5.3 An Attempt at Performing Transient Cycle

### *5.3.1 A Look at the Time Trace*

As previously mentioned, some time was taken during SETC software development to produce a transient test routine, and to see how well the test engine and dynamometer system would handle the Non-Road Transient Cycle [50]. Given the characteristics of the ODP, the dynamometer motor, and the engine's mechanical fuel rack, the routine was designed for operating the ODP in torque mode. To reiterate, when operating with torque control mode, the

ODP controls the dynamometer based on torque, instantly applying an input torque to motor5. The transient routine maintains speed with the fuel rack. Maintaining speed with the mechanical fuel rack of the test engine proved to be difficult, and there was noticeable lag between target speed, and measured speed. In some instances, the engine speed would oscillate significantly around a target speed while attempting to balance between maintaining enough speed at load, and too much fuel. Figure 46 below shows the comparison of speed output and target speed during the course of the transient cycle attempt.

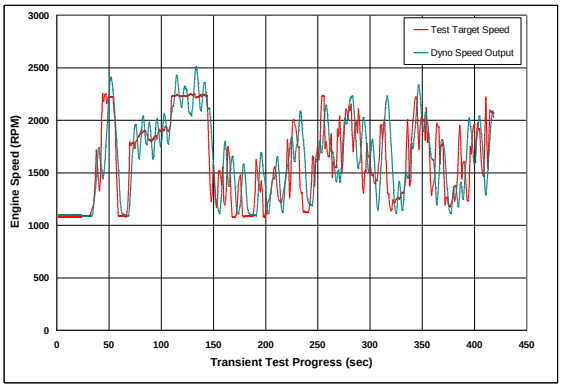


**Figure 46: Comparison of dynamometer speed output and target speed trace during transient test attempt.**

Obvious discrepancies are visible throughout much of the trace, and it is important to note that Figure 46 does not account for speed lag during the test. Despite this, one can assess from this plot that the mechanical fuel rack of the engine had significant trouble matching target speed during this trial test. The output speeds between the time of 75 seconds into the test and 150 seconds into the test show a clear oscillation of engine speed. During this time the fuel rack would increase too much and overshoot target speed, and account for this with too much fuel rack reduction. The ODP, on the other hand, was better able to match the target torque trace, as seen in Figure 47. While operating in torque mode, the ODP can immediately apply a target torque through the motor. There is some noticeable deviation at higher torque load set points.

The dynamometer fell short of these set points, which can be attributed to a torque limit that was set within the software code. At the time the transient test was performed, there were some reservations about allowing the dynamometer to exceed a torque of about 57 ft-lbs as it had shown to overload the motor at such high of a load. Later parameter changes to the controller relieved this issue, as can be seen with the steady state test cycle results, and it should not be an issue for future transient cycles to meet such high loads as 60 ft-lbs.

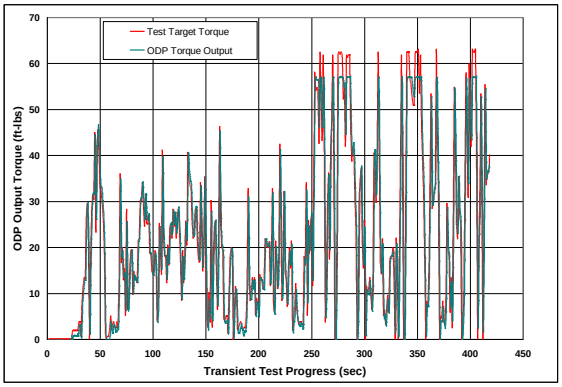


**Figure 47: Comparison of dynamometer torque output and target torque trace during transient test attempt.**

### *5.3.2 Cycle Validation with Torque Correlation*

A cross correlation was performed on both the speed and torque curves. As the torque curve closely follows the target torque trace, it had the best correlation, with the highest correlation constant occurring at the very beginning of the cycle indicating little to no time alignment necessary. The ODP torque output values are compared directly to the transient test target torque values in the following Figure 48**.**

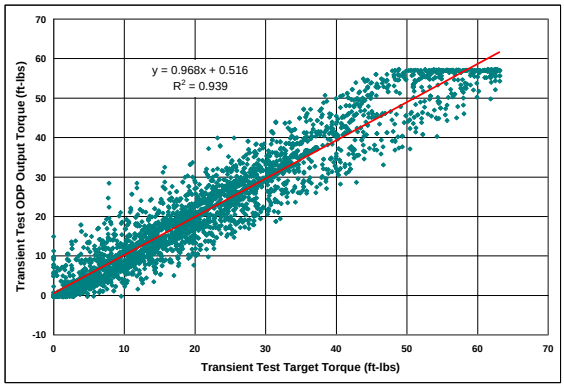


**Figure 48: Transient attempt ODP torque output compared directly to target torque values with no time alignment.**

Applying a linear trend line to the data shows a good agreement with a slope value close to one and an $r^2$ value close to one as well. However, with no time alignment there is noticeable deviation from the trend line. Figure 49 shows how the transient torque output points fall within 10, 25 and 50% of the target torque set point. Towards the lower end of the torque range the torque output points fall outside of up to ± 50% of the set point value, while the error improves towards the higher end of the torque set point range. A high torque values the majority of output points fall within ±25% of the set point value. CFR 1065.514 cycle validation criteria for a transient cycle are shown in Table 8.

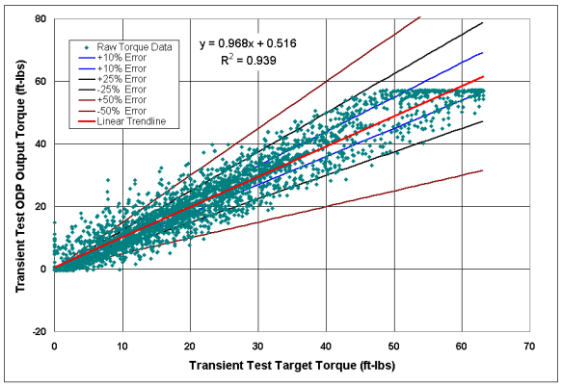


**Figure 49: Output to target value comparison with error lines.**

For the torque comparison, the linear equation shown in Figure 48 and Figure 49 has a slope value of 0.968, and an $r^2$ term of 0.939, both of which meet the CFR requirements for the

torque curve to pass cycle validation. The intercept of 0.516 is also less than 1.22 ft-lbs, which is 2% of the 61.1 ft-lbs of maximum mapped engine torque. The Standard Error of Estimate (SEE) for this torque data, when calculated using equation CFR 1065.602-11 is 6.41, and is slightly greater than 6.11, 10% of the maximum mapped torque value of 61.1 ft-lbs [45]. Given the SEE value, this torque data technically does not pass the CFR cycle validation criteria.

Continuing with the speed curve, and maintaining the same time alignment of the torque curve, the speed comparison between target speed and output speed is a completely different story. Figure 50 shows the obvious issues with agreement between target speed and output speed. It can be seen that the slope, intercept, and $r^2$ term of the linear trend line all fail the CFR cycle validation criteria of Table 8.

**Table 8: CFR 1065.514 Default statistical criteria for validating duty cycles [47].**

| Parameter | Speed | Torque | Power |
|---|---|---|---|
| Slope, $a_1$ | 0.950 ≤ a1 ≤ 1.030 | 0.830 ≤ a1 ≤ 1.030 | 0.830 ≤ a1 ≤ 1.030 |
| Absolute value of intercept, $a_0$ | ≤ 10% of warm idle | ≤ 2% of maximum mapped torque | ≤ 2% of maximum mapped power |
| Standard error of estimate, *SEE* | ≤ 5% of maximum test speed | ≤ 10% of maximum mapped torque | ≤ 10% of maximum mapped power |
| Coefficient of determination, $r^2$ | ≥ 0.970 | ≥ 0.850 | ≥ 0.910 |

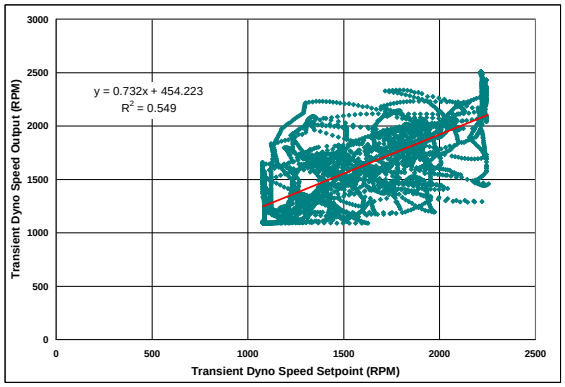


**Figure 50: Transient attempt speed output compared directly to target speed values with no time alignment.**

It is clear that time aligning the speed and torque feedback based on the close correlation between the output and target torque curves leads to cycle validation failure of the transient cycle

attempt. Though, as has been discussed, this is predominantly the fault of the issues with matching the target cycle speed and not so much matching that of the target torque curve.

### *5.3.3 Cycle Validation with Speed Correlation*

Perhaps, given the visible issues with the speed curve, it is necessary to base the time alignment of the speed and torque data on the correlation between the speed output and target speed values instead of that of the torque. The highest correlation constant with the speed feedback values was found to be at 4.5 seconds into the test data. Shifting the speed feedback data up 4.5 seconds for time alignment yields a new comparison plot, which is shown in Figure 51. However, despite time shifting the data based on the calculated cross correlation coefficient between the speed target values and the speed output values, the slope, intercept, and $r^2$ value all still fail to meet the cycle validation criteria.

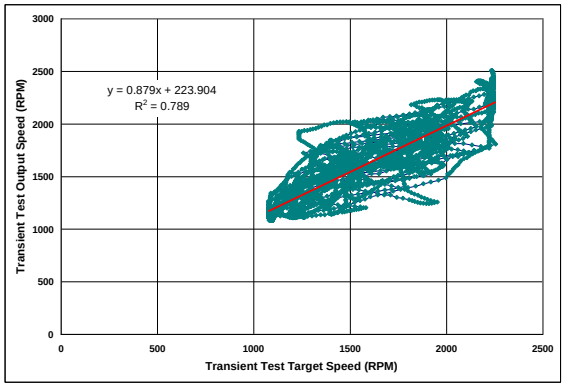


**Figure 51: Transient attempt speed output compared directly to target speed values with time shift of 4.5 seconds.**

It is important to recognize that this does not indicate that the SETC is incapable of operating a transient cycle. Experimentation with an electronically controlled engine, as well as improvements of the transient cycle software could go a long way towards improving the transient capabilities of the SETC. As the scope during commissioning of the SETC fell towards

steady state tests for capturing emissions with the lab, no further attempts at performing a transient test were made.

## 5.4 Test Engine Steady State Emissions Results

### *5.4.1 Notes on Emissions Results*

It should be noted prior to the emissions results, a deviation from the typical process of accounting for background emissions. Typically, background emissions are collected into a bag during the test, as previously discussed, and then sampled through the analyzers at the end of the test. Though this process was performed, following all tests, it was clear that not enough time between the end of the actual test, and taking the bag sample was given. Due to this, pollutants remaining within the sample lines from the last mode were sampled along with the background bag. This error resulted in significantly high gaseous emissions background data, which improperly offset the actual test data when correcting for background. However, each day prior to testing, a full twenty minute background test was performed to collect PM background data in which gaseous background data was also collected. Due to the poor background bag data collected during testing, the data collected during the background PM tests was used to correct the data from each day's tests for background.

### *5.4.2 Baseline*

The original test plan called for three baseline tests; however the data from four tests was kept. During Test B, no filter was placed in the PM box for PM collection; however the emissions data for this test was still good, and as a result is reported in the final results for further test comparison. The weighted brake specific engine out emissions for all baseline tests are shown below in Table 9. The blue numbers represent the average engine out emissions for the set

of baseline tests. No hydrocarbon data is listed for Test A due to an issue with over ranging of the analyzer during the test. For the remaining tests, the HC analyzer was recalibrated with a more appropriately concentration propane bottle.

Figure 52 shows an example of the continuous engine out emissions concentration within the dilution tunnel for each sampled pollutant over the full test cycle, Test D. This continuous plot gives a good representation of the mode-specific emissions over the span of a full steady state test.

**Table 9: Baseline weighted engine out emissions.**

| Test | A | B | C | D | Average | Uncertainty | St Dev | 95% |
|---|---|---|---|---|---|---|---|---|
| | Weighted (g/bhp-hr) | | | | | ± | | Conf. |
| HC | - | 4.14 | 4.37 | 4.43 | 4.31 | 0.13 | 0.16 | 0.18 |
| CO | 3.08 | 2.52 | 2.56 | 2.69 | 2.71 | 0.13 | 0.25 | 0.25 |
| $CO_2$ | 797.83 | 746.06 | 715.63 | 748.39 | 751.98 | 24.63 | 34.02 | 33.34 |
| $NO_x$ | 7.73 | 7.36 | 7.02 | 7.22 | 7.33 | 0.25 | 0.30 | 0.29 |
| PM | 0.685 | - | 0.535 | 0.555 | 0.591 | 0.0105 | 0.0813 | 0.0920 |

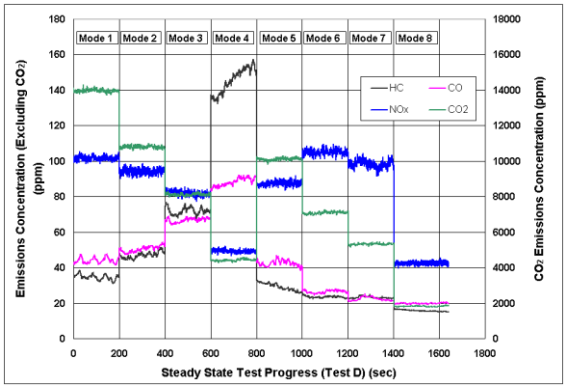


**Figure 52: Continuous engine out emissions data for baseline Test D.**

### *5.4.3 Controlled Tests with Catalyst-Layered Diesel Particulate Filter*

Weighted brake specific engine out emissions for the series of tests performed with a passive regeneration catalyst-layered DPF. Emissions results for the controlled tests can be found in Table 10. Figure 53, shows the continuous engine out emissions concentration for each pollutant over the full cycle of after treatment controlled Test F.

**Table 10: DPF Controlled weighted engine out emissions.**

| Test | E | F | G | Average | Uncertainty | St Dev | 95% |
|---|---|---|---|---|---|---|---|
| | Weighted (g/bhp-hr) | | | | ± | | Conf. |
| HC | 1.01 | 0.74 | 0.73 | **0.83** | 0.03 | 0.16 | 0.18 |
| CO | 0.55 | 0.38 | 0.36 | **0.43** | 0.03 | 0.11 | 0.12 |
| $CO_2$ | 809.22 | 806.61 | 818.15 | **811.33** | 25.59 | 6.05 | 6.85 |
| $NO_x$ | 7.29 | 7.28 | 7.25 | **7.27** | 0.24 | 0.02 | 0.03 |
| PM | 0.0981 | 0.0581 | 0.0878 | **0.0813** | 0.0022 | 0.0207 | 0.0235 |

Looking at the HC and CO traces in Figure 53 between the time of 600 and 800 seconds (test mode 4), one can observe a noticeable increase in both HC and CO during the progressions of mode 4. A DPF with a catalyst layer is a temperature-dependent device, with capabilities in pollutant reduction increasing with higher temperatures. Outside of the idle mode, mode 4 has the lowest load, at only 6 ft-lbs at 2200 rpm, and the decrease in exhaust temperature over this low load interval allowed for a decrease in DPF temperature. As the temperature of the DPF decreased, its ability to reduce the emissions of HC and CO dropped significantly. This drop in DPF emission reduction during mode 4 could have been prevented had the mode been lengthened, allowing for adequate temperature stabilization of the DPF. Figure 54 shows the continuous emission concentrations of HC and CO during the entirety of Test F as well as exhaust temperature, which was recorded directly after the DPF, to illustrate how reduction of HC and CO was affected by exhaust temperature.

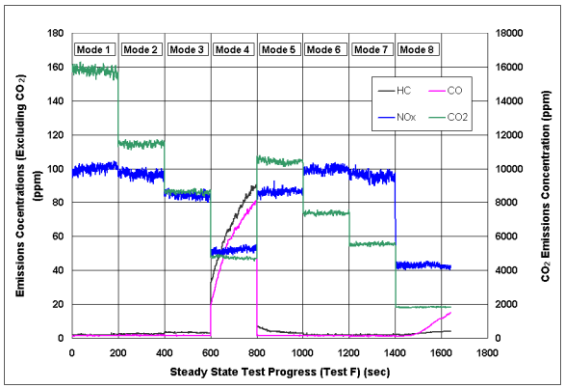


**Figure 53: Continuous engine out emissions data for baseline Test F.**

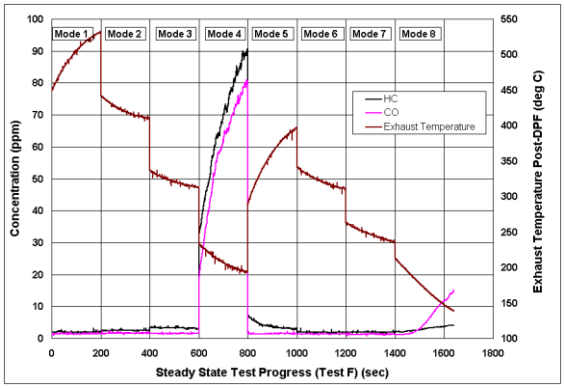


**Figure 54: Controlled Test F continuous HC and CO compared to post-DPF exhaust temperature.**

### *5.4.4 Comparison of Baseline and Controlled Test Results*

The addition of the DPF resulted in reductions in average engine out emissions of PM, HC, and CO emissions of 86%, 81%, and 84% respectively. HC and CO were reduced by the catalyst layer, and PM reduction was due filtration and capture through the DPF [39]. Figure 56, through Figure 55 and Table 11 show the direct comparison between the baseline and controlled emissions of these three significantly reduced pollutants.

**Table 11: Comparison between baseline and controlled tests.**

| Species | Baseline Average (g/bhp-hr) | Controlled Average (g/bhp-hr) | Delta (%) |
|---|---|---|---|
| HC | 4.31 | 0.83 | -81 |
| CO | 2.71 | 0.43 | -84 |
| $CO_2$ | 751.98 | 811.33 | 8 |
| PM | 0.59 | 0.08 | -86 |

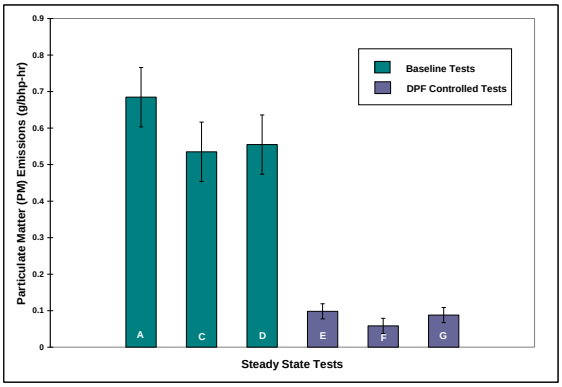


**Figure 55: Comparison of total weighted PM emissions for all tests.**

The reduction results of PM, HC, and CO found when using the DPF, are consistent with other experimental results in DPF exhaust emission reduction. A recent series of experimental tests on a similar, yet significantly newer engine, and similar DPF, preformed by the CAFEE group here at WVU showed reduction results for PM, HC, and CO of 98%, 75%, and 64% respectively [51]. Another similar on more heavy duty diesel engines with a DPF performed by Cummins Emissions Solutions and the University of Wisconsin-Madison, showed reduction results of HC, CO, and PM of approximately 78%, 90%, and 95% respectively [39]. For the controlled tests, $CO_2$ was slightly increased by 8% over the baseline tests. This result can be attested to the increased exhaust backpressure caused by the DPF itself, as well as some regeneration of PM within the DPF.

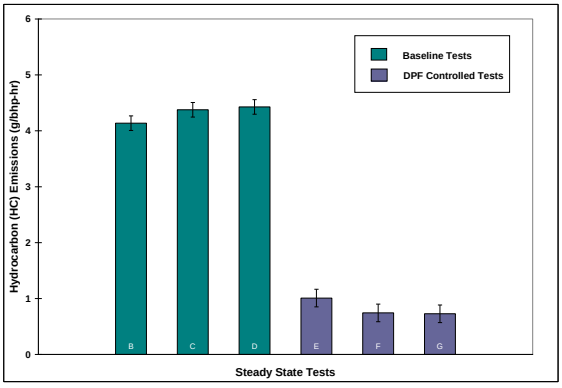


**Figure 56: Comparison of total weighted HC emissions for all tests.**

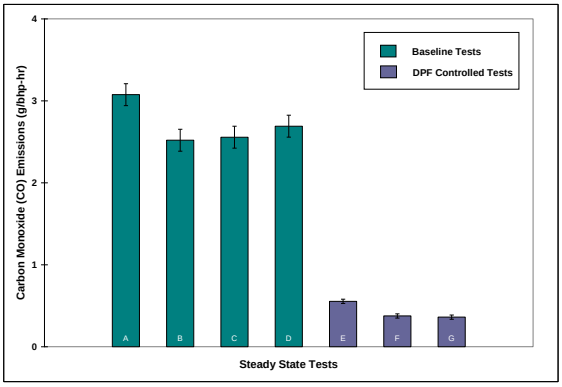


**Figure 57: Comparison of total weighted CO emissions for all tests.**

### 5.4.5 *Carbon Balance*

As no previous data exists for this particular engine, and detailed results from CAFEE testing of a similar engine are unavailable for comparison, the most accurate method of describing the validity of the data presented was a carbon balance between the carbon within the fuel consumed and that measured within the exhaust gases. The weighted average carbon balance results from each test are given in Table 12. The carbon balance shows good agreement between the carbon consumed from the fuel, and that from the exhaust, with all exhaust carbon rates within 5% of the fuel carbon rates. The carbon rate from the fuel was calculated from the measured diesel fuel flow rate, and the carbon rate in the exhaust was calculated from the measured concentrations of HC, CO, and $CO_2$ in the dilute exhaust mixture.

**Table 12: Comparison of carbon contained within the fuel consumed to the carbon measured within the exhaust.**

| Average Weighted Carbon Balance | | | | | | | |
|---|---|---|---|---|---|---|---|
| **Test** | **A** | **B** | **C** | **D** | **E** | **F** | **G** |
| Carbon from Diesel Flow (kg/hr) | 2.66 | 2.50 | 2.48 | 2.56 | 2.62 | 2.70 | 2.69 |
| Carbon Measured in Exhaust (kg/hr) | 2.77 | 2.55 | 2.45 | 2.56 | 2.72 | 2.71 | 2.74 |
| % Difference | +4.28 | +2.05 | +1.31 | +0.20 | +4.01 | +0.28 | +1.79 |

### 5.4.6 *Rounding, Error, and Statistical Analysis*

CFR Title 40, Part 1065.20 states that with the reporting of results, values should be rounded to the number of significant digits necessary to match the number of decimal places of the standards applicable to the result [45]. As the standards for emissions associated with the testing of a TRU are predominantly listed to two decimal places, the majority of results have been listed as such. However, there are some instances where results are reported to further decimal places than necessary. All PM matter has been reported to three significant figures to better suit those who may use the content within this document as a comparison to future results.

Likewise, the standard listed in the upcoming sections comparing results lists the CO standard to one decimal place. In this case, the previously stated two decimal place rule for this document still applies.

In an effort to quantify the experimental error associated with the collection and calculation of the weighted brake specific engine out emissions of the SETC engine, an error analysis was performed. During this analysis, it was assumed first that the uncertainty of the analyzers and flow meters was 2% of the measured value [0]. Error propagation from data collection to final calculation was performed using the overall error calculation Equation 14 [59].

$$Err = \sqrt{\left[\left[\Delta u_1 \frac{\partial f}{\partial u_1}\right]^2 + \left[\Delta u_2 \frac{\partial f}{\partial u_2}\right]^2 + \ldots + \left[\Delta u_n \frac{\partial f}{\partial u_n}\right]^2\right]} \qquad \text{Equation 14}$$

Where,

***Err*** = Overall uncertainty propagation through the final calculation

***f*** = Function of $u$ as: $f = f(u_1, u_2, \ldots, u_n)$

***Δu*** = Associated error of a component or instrument used in the final calculation

$\frac{\partial f}{\partial u}$ = The partial derivative of $f$, evaluated at $u$

This equation was applied to each step in the final calculation for weighted brake specific engine out emissions of HC, CO, $CO_2$, $NO_x$, and PM. An example of this error propagation calculation is given below in Equation 15 for calculating total power for one mode of a steady state cycle.

$$\dot{E} = \frac{N \times \tau}{5252} \qquad \text{Equation 15}$$

Where,

$\dot{E}$ = Total power for a specific steady state mode in (bhp) (kW)

$N$ = Average engine speed recorded during the mode in (RPM)

$\tau$ = Average engine output torque recorded during the mode in (ft-lbs) (N-m)

5252 = Engineering simplification constant, incorporating the conversion of RPM to (rad/s), and (ft-lb)/s into (hp).

As the 2% assumption did not apply to these items, three standards of deviation were used as the uncertainty, u, for both speed and torque. Using the data from Test A for this example this lead to an uncertainty in speed for mode 1 of 2220±14.50 RPM, and an uncertainty for torque of the same mode as 63±0.64 ft-lbs. Applying the equation for overall error to the power calculation, the resulting Equation 16 becomes

$$Err = \sqrt{\left[\left[\Delta N \frac{\partial \dot{E}}{\partial N}\right]^2 + \left[\Delta T \frac{\partial \dot{E}}{\partial \tau}\right]^2\right]} \qquad \text{Equation 16}$$

When applied to the actual data values, the above equation results in a total error for the calculation of power during mode 1 of Test A of ±0.32 hp. This same practice was applied to all equations leading up to and including the total weighted brake specific engine out emissions for the engine for each test. Total emissions for each test were compared to the remaining tests of similar setup, whether baseline, or controlled. Standard deviations were also calculated between tests, A, B, C, and D, as well as between E, F, and G. Refer again to Table 9 and Table 10 for the standard deviation values. For the purposes of the data reported in this document, it was assumed

that the largest uncertainty associated with an emission result, whether the calculated error propagation through the calculation, or the standard deviation when compared to a similar calculated value, the larger of the two would be reported. The largest of these values for an emission result error was used to apply error bars to all plots describing the weighted brake specific engine out emissions for each pollutant of each test.

### *5.4.7 Main Tunnel Dilution Ratio*

Per CFR Title 40 part 1065.140 the minimum dilution ratio within the main dilution tunnel must be at least 2:1 [45]. Total dilution ratio is based on the exhaust flow into the dilution tunnel, and dilution air flow into the tunnel. The diagram in Figure 58 shows the aspects of the dilution system used in commissioning of the SETC.

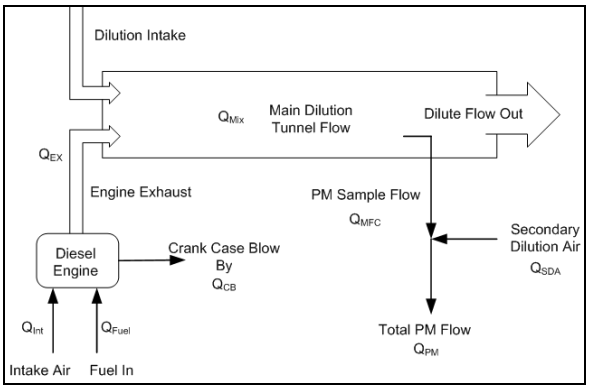


**Figure 58: SETC commissioning dilute system diagram.**

The system simplifies to Equation 17.

$$\frac{Q_{Mix} - Q_{Ex}}{Q_{Ex}} \qquad \text{Equation 17}$$

Where,

$Q_{Mix}$ = the total measured dilution flow rate in ($ft^3$/min) ($m^3$/s)

$Q_{Ex}$ = the exhaust flow rate into the dilution tunnel in ($ft^3$/min) ($m^3$/s)

Looking further into $Q_{Ex}$, it is clear that this is the sum of the intake air, fuel consumption, and crankcase blow-by out. This sum is clarified in Equation 18.

$$Q_{Ex} = Q_{Int} + Q_{FC} - Q_{CB} \qquad \text{Equation 18}$$

Where,

$Q_{Int}$ = the engine intake air flow rate in ($ft^3$/min) ($m^3$/s)

$Q_{FC}$ = the fuel flow into the engine fuel rack ($ft^3$/min) ($m^3$/s)

Given that, while certainly existing, both fuel consumption, and crankcase blow-by are minimal when compared to intake air for this engine, it is acceptable to assume, for the purposes of simplification that these two elements of the equation are essentially zero. The equation for $Q_{Ex}$ then simplifies to,

$$Q_{Ex} = Q_{Int} \qquad \text{Equation 19}$$

Finally, this leads to the simplified equation for dilution ratio.

$$\frac{Q_{Mix} - Q_{Int}}{Q_{Int}} \qquad \text{Equation 20}$$

Average overall dilution ratios for each mode of each test are tabulated below in Table 13. As these calculated approximate dilution ratios for each mode are between the ranges of 6:1 to 12.5:1, the requirement of a minimum 2:1 has certainly been met. Dilutions ratios of this range

are moderately high for the main dilution tunnel system, however, due to the level of pollutants produced, by such an older, poor condition engine, such as the Isuzu CP-201 used during testing, this range of dilution ratio is preferred to prevent any detrimental affects to system analyzers, and to ensure good measurements.

**Table 13: Average overall tunnel dilution ratios during each test.**

| Main Tunnel DR | | | | | | | | |
|---|---|---|---|---|---|---|---|---|
| Test | Mode | | | | | | | |
| | 1 | 2 | 3 | 4 | 5 | 6 | 7 | 8 |
| A | 6.30 | 6.07 | 6.06 | 5.86 | 9.42 | 9.78 | 8.81 | 12.14 |
| B | 6.18 | 6.01 | 5.91 | 5.75 | 9.14 | 9.00 | 8.70 | 12.01 |
| C | 6.17 | 6.13 | 5.96 | 5.75 | 9.95 | 9.81 | 9.19 | 12.13 |
| D | 6.16 | 6.09 | 5.90 | 5.75 | 9.04 | 8.99 | 9.07 | 12.09 |
| E | 6.30 | 6.10 | 6.01 | 5.84 | 9.53 | 7.14 | 9.00 | 12.30 |
| F | 6.34 | 6.25 | 6.06 | 5.84 | 9.16 | 8.95 | 9.01 | 12.31 |
| G | 6.41 | 6.24 | 6.09 | 5.86 | 9.55 | 9.24 | 9.11 | 12.42 |

### *5.4.8 Effect of Omitting Secondary Dilution*

As mentioned previously, time and funding constraints lead to the omission of secondary dilution air from the PM sampling system. Again, the main purpose of using secondary dilution air during PM sampling is to maintain filter face temperature at the required level of 117 ±11 °F, and maintain a minimum dilution ration of between 5:1 and 7:1 through the PM system [45]. Table 14 shows the average filter face temperature from each test, as well as its deviation from the CFR 1065 requirement [45].

**Table 14: Average filter face temperatures compared to required.**

| Test No. | Average FF Temp. (°F) | Req'd Per CFR (°F) | % Difference |
|---|---|---|---|
| A | 119.16 | 117 | 1.81% |
| B | 119.12 | 117 | 1.78% |
| C | 117.36 | 117 | 0.30% |
| D | 118.99 | 117 | 1.67% |
| E | 118.99 | 117 | 1.67% |
| F | 118.78 | 117 | 1.49% |
| G | 118.69 | 117 | 1.42% |

As one can see, despite the lack of secondary dilution air, filter face temperatures remained within 2% of the required temperature. This is not an attempt to provide data against the use of secondary dilution air; it is only to show what was affected during this specific testing

series. With regard to PM system dilution ratio, the minimum ratio of 5:1-7:1 was more than met, perhaps somewhat excessively, as the PM sample flow mass flow controller (MFC) was set to maintain a flow rate of 1 scfm. Initially, during the first trial run attempts, PM flow was set to 2.5 scfm. Due to the amount of soot produced by this dirty engine, at 2.5 scfm, the PM was heavy on the filter, and there was fear over overloading the filter. It was suggested that for further attempts, the PM MFC should be set at 1 scfm, where it remained for all subsequent tests. Looking at the PM system of the diagram in Figure 58, the equation necessary to calculation the dilution ratio of the PM system, similar to that of the main tunnel dilution ratio is simply,

$$\frac{Q_{Mix} - Q_{PM}}{Q_{PM}} \qquad \text{Equation 21}$$

Where,

$Q_{PM}$ = the total flow rate sum of the PM MFC, and the secondary dilution air flow, as described in Equation 22.

$$Q_{PM} = Q_{MFC} + Q_{SDA} \qquad \text{Equation 22}$$

Where,

$Q_{SDA}$ = the flow rate of secondary dilution air within the PM system in ($ft^3$/min) ($m^3$/s)

$Q_{MFC}$ = the flow through the PM mass flow controller in ($ft^3$/min) ($m^3$/s)

Again, as secondary dilution air has been omitted from the PM sampling system $\dot{Q}_{SDA}$ is zero, simplifying the PM dilution ratio equation to that of Equation 23.

$$\frac{Q_{Mix} - Q_{MFC}}{Q_{MFC}}$$ Equation 23

PM dilution ratios were all approximately 400:1 for each test. Despite being most likely being an over-dilute situation, particulate matter loading on all filters was still adequate for providing results. Table 15 displays the average dilution ratios for the PM. system

**Table 15: Average dilution ratios for the PM system during all tests.**

| PM System DR | | | | | | | | |
|---|---|---|---|---|---|---|---|---|
| Test | Mode | | | | | | | |
| | 1 | 2 | 3 | 4 | 5 | 6 | 7 | 8 |
| A | 398.89 | 398.99 | 399.03 | 399.06 | 398.95 | 399.00 | 399.03 | 399.01 |
| B | - | - | - | - | - | - | - | - |
| C | 398.91 | 398.95 | 399.01 | 399.04 | 398.98 | 399.03 | 398.98 | 399.02 |
| D | 398.90 | 399.00 | 399.03 | 399.05 | 398.95 | 399.05 | 399.04 | 399.02 |
| E | 398.92 | 398.98 | 399.05 | 399.03 | 399.00 | 399.01 | 399.02 | 399.06 |
| F | 399.03 | 398.95 | 399.02 | 399.04 | 398.99 | 399.00 | 399.02 | 399.01 |
| G | 398.92 | 398.96 | 399.05 | 399.02 | 398.99 | 398.96 | 399.02 | 399.02 |

## 5.5 Comparing Results to Engine Model Year Emissions Standards

Having gathered the appropriate data with the SETC and performed the proper calculations for weighted brake specific emissions, it was necessary to compare the results with the applicable emission requirements of the engine used during testing. First, refer back to Table 9 and Table 10 for all engine-out weighted particulate matter emissions.

### *5.5.1 Particulate Matter Emissions Compared to Standards*

With a TRU engine, such as the Isuzu CP-201 used during commissioning of the SETC, the main concern with emissions regulations at this time is PM. Referring back to Section 2.9, the CARB is introducing PM emissions requirements for all TRUs operating within California borders, at different levels and dates, depending upon model year and size of the TRU engine. The resulting average total particulate matter emissions for the test engine for both all baseline

and controlled tests were found to be 0.591 and 0.0813 (g/bhp-hr) respectively. CARB is also requiring currently, as of its recent Final Regulation Order [2] that TRU engines of greater than 25 hp must meet the Low-Emissions In-Use Performance Standards by December 31, 2009, and must meet the Ultra Low-Emissions standards by 2015. At this current time, this ~1986 model year engine falls under the Low-Emissions requirement of 0.22 (g/bhp-hr) with a minimum level 2 VDECS resulting in a PM reduction of greater than 50%. These standards for all TRU engines for model year 2002 and older will begin being enforced as of January 2010. With the DPF in place, the SETC test engine produced a weighted engine out total particulate emission of 0.08134 (g/bhp-hr) with a result of 86% PM reduction. This result supports the assessment that, with the DPF used during testing; the SETC Isuzu CP-201 engine does in fact meet CARB's current Low-Emission In-Use Performance Standard. With the 86% reduction in PM, the DPF has also just barely met the level 3 VDECS as well as level 2. Table 16 summarizes the PM results of the test engine.

**Table 16: Test engine PM results compared to CARB PM requirements for TRUs.**

| | | CARB LETRU Standard | | |
|---|---|---|---|---|
| Test Condition | Average PM Emissions (g/bhp-hr) | PM Emission Requirement (g/bhp-hr) | Min. VDECS Level | Pass/Fail |
| Baseline | 0.591 ± 0.011 | 0.22 | 2 | Fail |
| Controlled | 0.0813 ± 0.0022 | 0.22 | 2 | Pass |

### *5.5.2 Gaseous Emissions Results Compared to Standards*

As the Isuzu CP-201 tested was manufactured in the middle 1980's, no specific EPA emissions regulations could be found for this particular nonroad diesel engine. EPA Tier 2 standards for non-road compression ignition engines of between 25 and 50 horsepower apply to model years of 2004 and later, and Tier 1 standards go only as far back as 1999 model year engines [59]. The EPA Title 40, Part 1039, which applies specifically to new and in-use non-road

compression ignition engines, excludes this particular engine as it is below 50 hp [54]. However, if an engine of this nature were to be verified with the SETC, certain standards would apply. For the sake of process, EPA Tier 1 and 2 requirements will be applied to the baseline and controlled results for engine out emissions of the Isuzu CP-201. These requirements and results of comparison to the engine tests are summarized below.

**Table 17: Tier 1-2 Non Road Diesel Engine Emissions Standards [50]**

| EPA Requirements For Nonroad CI Engines of 25 ≤ hp ≤ 50 (g/bhp-hr) | | | | | |
|---|---|---|---|---|---|
| Tier | Year | CO | HC | NOx | PM |
| 1 | 1999 | 4.1 | - | - | 0.6 |
| 2 | 2004 | 4.1 | - | - | 0.45 |

Again, even when applying the EPA standards of later model year similar engines, no requirements are in place for HC and $NO_x$. Looking at CO and PM however, both Tier 1 and 2 standards can be applied to the Isuzu engine tested. From Table 9 and Table 10 the baseline average result for CO was 2.71 (g/bhp-hr) and 0.591 (g/bhp-hr) for PM. The baseline results meet Tier 1 and 2 standards for CO and the Tier 2 standard for PM. The baseline PM however just barely meets the Tier 1 PM standard. Similarly the controlled average results of 0.43 (g/bhp-hr) for CO and 0.0813 (g/bhp-hr) for PM comply with both the Tier 1 and 2 standards for CO and PM. With an after treatment device, even an older model engine, such as the Isuzu CP-201 used in commissioning of the SETC, can meet the standards of later model year engines. Once more, applying these standards to this engine is merely an exercise, as there are no specific gaseous emissions standards for older Non road diesel engines, such as a TRU engine.

### *5.5.3 Engine NO and $NO_2$ Emissions, Issues, and Concerns*

As of January 1, 2009, along with the PM reduction requirements, CARB is also requiring that any diesel emission control strategy (DECS) does not increase $NO_2$ emission levels more than 20% over that of the baseline emissions [56]. CARB will, however, state that

any DECS installed prior to the compliance date that does not comply with the less than 20% $NO_2$ increase requirement is to be considered "unverified" and allowed to remain in service as fleet rule compliance candidates, and cannot be installed or sold as "verified" [57].

A claim of compliance with this requirement, or non-compliance as well, cannot be made for the aftertreatment device used during SETC commissioning. The NO, and resulting $NO_2$, emissions data collected during testing are flawed in that the results show $NO_2$ accounting for almost 80% of all $NO_x$ emissions for the baseline and controlled tests. For typical diesel engines, $NO_2$ should make up no more than 10 to 30% of the total baseline $NO_x$ emissions [58]. Figure 59 shows the difference between the continuous $NO_x$ and NO data from the analyzers during all baseline tests. From this plot, it was apparent that there was an issue with the NO data, as it was significantly lower than the $NO_x$ emission concentration trace line, representing higher levels of $NO_2$ than expected. One of the more unusual aspects of these results was that the matter of the NO data appears consistently for all baseline tests. Further detailed emissions results based on these questionable data will not be provided in this document to prevent any misleading of the reader.

While the controlled results showed an expected, though slight, overall increase in $NO_2$ emissions, the significant gap between $NO_x$ and NO emissions remained. The continuous results of $NO_x$ and NO for the three controlled tests, which are similar to that of the baseline, are shown in Figure 60. For the controlled tests, the NO continuous trace is noticeably different than that of the baseline tests; however, it still remained unusually lower than the NOx data, furthering the concern with the data.

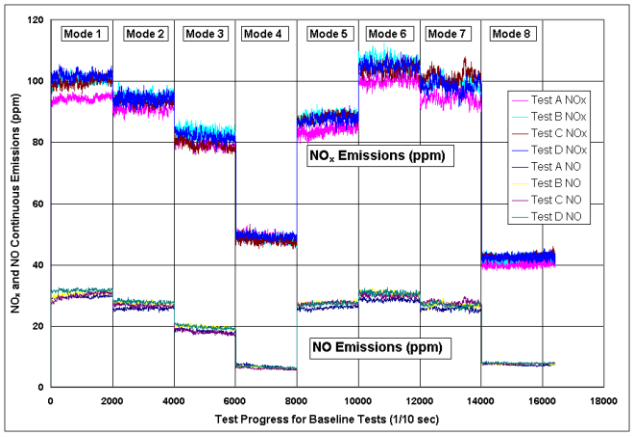


**Figure 59: Atypical results for continuous NOx and NO concentrations for all baseline tests (A-D).**

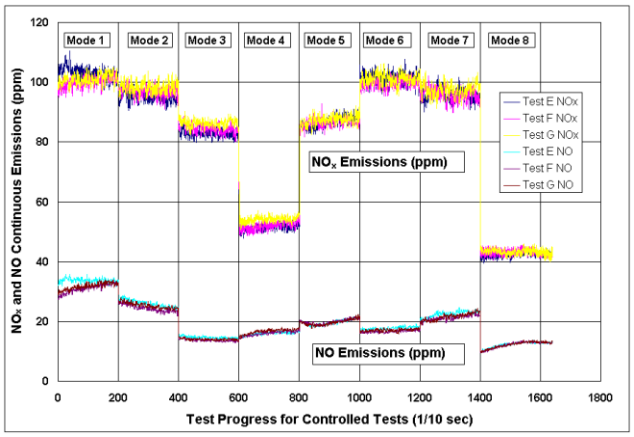


**Figure 60: Atypical results for continuous NOx and NO concentrations for all DPF controlled tests (E-G).**

The first possible thought was that this was a reduction and calculation issue, and so the reduced data that was produced with the SETC Microsoft Visual Basic reduction software was then compared to that of the Data Viewer 2007 software within the mobile analytical trailer itself, and the same continuous results were found. The problem is also consistent for all tests, baseline and controlled. Both $NO_x$ analyzers were in proper working order during tests, both were calibrated properly prior to testing, and a recent $NO_x$ converter efficiency test had also been performed with $NO_x$ converter efficiencies for both analyzers above 90%. A test was never performed with both analyzers operating in NOx mode to compare that they were both reading properly, and as such, cannot be used to support or deny these results. Other possible reasons for

the strange nature of the NO and $NO_2$ data are that there may have been an internal leak in the CAI 600 analyzer allowing ambient air to affect the reading, or that that the CAI 600, while operating in NO mode, was in an incorrect range for properly recording data. Had the analyzer been operating in an inappropriate range, this could explain the consistency in the poor results.

As the objective of the series of the SETC tests on the Isuzu CP-201 was to show the working capabilities of the SETC, and not to verify the DPF aftertreatment device used, these questionable results do not invalidate the scope work documented, only the NO and $NO_2$ data. It is, however, the suggestion of the author, that for any future emissions tests with the Isuzu CP-201, any $NO_x$, NO, and $NO_2$ data collected be checked carefully to see if there are any discrepancies regarding NO and $NO_2$.

# Chapter 6: Conclusions and Recommendations

# 6 Conclusions and Recommendations

## 6.1 Conclusions

Emissions data were collected and summarized from a 1986 Isuzu CP-201 27 horsepower 4-cylinder diesel engine over an 8-mode ISO 8178 steady state test cycle for both baseline and DPF controlled emissions in order to prove the overall concept of the lab. Once more, all results for the steady state SETC commissioning tests, including test cycle validation, weighted brake specific engine-out emissions, and compliance with existing emissions standards, have been tabulated in Table 18, Table 19, and Table 20. The numbers in red signify a specific mode within a test that failed to meet the cycle validation criteria.

**Table 18: Speed cycle validation summary**

| Test | Average Deviation From Reference Speed (% Difference) Mode | | | | | | | Cycle Validation |
|---|---|---|---|---|---|---|---|---|
| | 1 | 2 | 3 | 4 | 5 | 6 | 7 | % of Ref. |
| A | 11.23 | 0.10 | 0.02 | 0.06 | 0.42 | 0.08 | 0.11 | ≤ 2% |
| B | 0.07 | 0.15 | 0.03 | 0.09 | 0.32 | 0.06 | 0.13 | ≤ 2% |
| C | 0.03 | 0.12 | 0.04 | 0.07 | 0.30 | 0.08 | 0.11 | ≤ 2% |
| D | 0.05 | 0.08 | 0.08 | 0.06 | 0.22 | 0.12 | 0.10 | ≤ 2% |
| E | 0.12 | 0.11 | 0.04 | 0.13 | 0.38 | 0.07 | 0.12 | ≤ 2% |
| F | 0.22 | 0.06 | 0.02 | 0.04 | 0.42 | 0.10 | 0.02 | ≤ 2% |
| G | 0.19 | 0.06 | 0.07 | 0.18 | 0.30 | 0.10 | 0.17 | ≤ 2% |

**Table 19: Torque cycle validation summary**

| Test | Average Deviation From Reference Torque (% Difference) Mode | | | | | | | Cycle Validation |
|---|---|---|---|---|---|---|---|---|
| | 1 | 2 | 3 | 4 | 5 | 6 | 7 | % of Ref. |
| A | 3.50 | 0.40 | 0.60 | 3.37 | 1.48 | 0.40 | 0.60 | ≤ 2% |
| B | 0.34 | 0.38 | 0.60 | 3.17 | 4.22 | 0.40 | 0.61 | ≤ 2% |
| C | 0.33 | 0.39 | 0.62 | 7.14 | 5.08 | 0.40 | 0.61 | ≤ 2% |
| D | 0.32 | 0.41 | 0.62 | 1.82 | 3.62 | 0.40 | 0.61 | ≤ 2% |
| E | 0.31 | 0.39 | 0.62 | 3.39 | 1.84 | 0.40 | 0.64 | ≤ 2% |
| F | 0.33 | 0.40 | 0.60 | 3.52 | 1.58 | 0.40 | 0.60 | ≤ 2% |
| G | 0.33 | 0.40 | 0.62 | 3.59 | 0.56 | 0.38 | 0.62 | ≤ 2% |

The series of steady state tests that were performed during this commissioning study have shown that the SETC is functional and able to perform testing on small engines for CAFEE in the future. A few aspects requiring further attention, when the time comes, are mentioned in the

following Section 6.2. As an overall system, the lab has been shown to have the ability to hold desired speed and load, follow a desired steady state test cycle, and be used in conjunction with emissions measurement systems to perform emissions studies on small engines and exhaust aftertreatment devices.

**Table 20: Emissions results final summary**

| Baseline Tests | A | B | C | D | Average | Emissions Standard | | |
|---|---|---|---|---|---|---|---|---|
| | Weighted (g/bhp-hr) | | | | | CARB LETRU | EPA Tier 1 | EPA Tier 2 |
| HC | - | 4.14 | 4.37 | 4.43 | 4.31 | - | - | - |
| CO | 3.08 | 2.52 | 2.56 | 2.69 | 2.71 | - | Pass | Pass |
| $CO_2$ | 797.83 | 746.06 | 715.63 | 748.39 | 751.98 | - | - | - |
| $NO_x$ | 7.73 | 7.36 | 7.02 | 7.22 | 7.33 | - | - | - |
| PM | 0.685 | - | 0.535 | 0.555 | 0.591 | Fail | Pass | Fail |
| Controlled Tests | | E | F | G | Average | Emissions Standard | | |
| | | Weighted (g/bhp-hr) | | | | CARB LETRU | EPA Tier 1 | EPA Tier 2 |
| HC | | 1.01 | 0.74 | 0.73 | 0.83 | - | - | - |
| CO | | 0.55 | 0.38 | 0.36 | 0.43 | Pass | Pass | Pass |
| $CO_2$ | | 809.22 | 806.61 | 818.15 | 811.33 | - | - | - |
| $NO_x$ | | 7.29 | 7.28 | 7.25 | 7.27 | - | - | - |
| PM | | 0.0981 | 0.0581 | 0.0878 | 0.0813 | Pass | Pass | Pass |

## 6.2 Recommendations

### *6.2.1 Hardware Recommendations*

It is the recommendation of the author, that with the conception of future funded projects involving the SETC, that the appropriate time and funds be spent to provide a proper cooling fan to be mounted with the cooling system's radiator. The same should be applied to the fuel conditioning box within the SETC. Having a fully functioning fuel conditioning system to maintain fuel temperatures would provide the SETC with a more stable fuel system, like that of the test cell in the ERC. It is also suggested that for future applications, an inline torque sensor with a more appropriate measurement range, be installed. A range of 0 to 200 ft-lbs would work well if available.

### *6.2.2 Cycle refinement*

As was mentioned in Sections 5.2 and 5.3 of this document, the SETC is appropriately capable of operating a steady state test cycle, and has also shown the possibility of performing transient cycles as well. There remains some room for improvement within the steady state cycle software, specifically with regard to the operation used in control of mode 5. Whether it was solely the fault of the engine not being able to hold the intended speed and load well during mode 5, or an issue with the software itself, remains to be determined. However, at this time, with the software currently in place, handing over full control of the dynamometer to the Smarty operating in speed mode was the best method of handling mode 5. With more time, the software could be properly tuned to operate mode 5 in the same manner as all other modes, and different engines are also likely perform differently than the current test engine.

Likewise, with the transient cycle, more time spent fine-tuning control software, as well as an appropriately electronic fuel rack controlled engine could produce more substantial proof of the SETC's ability to run a transient routine. Again, the results of the transient cycle attempt shown in section 5.3 suggest that the SETC could, in time, be used for transient operation.

# 7 References


1. Regulatory Advisory November 2005, Advisory 05-01, California Air Resources Board, November 2005.

2. California Air Resources Board (CARB) Final Regulation Order, "Airborne Toxic Control Measure for In-Use Diesel Fueled Transport Refrigeration Units (TRU) and TRU Generator Sets, and Facilities Where TRUs Operate." www.arb.ca.gov. (Accessed June 8, 2008).

3. Broder, J.M., Baker, P., "Obama's Order Is Likely to Tighten Auto Standards." The New York Times 25 January 2009. http://www.nytimes.com/2009/01/26/us/politics/26calif.html. (Accessed February 20, 2009).

4. Grupp, D., Dwyer, H. A., Kulkarni, C., Solomon, M., Miller, M., "Design, Testing, and Demonstrating of a Hybrid Fuel Cell Powered APU/TRU System," University of California-Davis, SAE paper 2007-01-0699, 2007.

5. Mader, P., Kulkarni, C., and Dwyer, H. A, Brodrick, C.J.., "Emissions Performance, and Duty Cycle Measurements of Diesel Powered TRUs," University of California-Davis, SAE paper, 2007-01-1087, 2007.

6. The American Society of Mechanical Engineers, "The Thermo King Model C Transportation Refrigeration Unit, an International Historic Mechanical Engineering Landmark," ASME International, October 1, 1996.

7. Thermo King Corporation refer unit image. Thermo King http://www.thermoking.com/tk/index.asp. (Accessed February 25, 2009).

8. SmartWay Transportation Partnership. (2004) Idle Free Corridors: Implementation Meeting. http://epa.gov/smartway/presentations/background.pdf48. (Accessed March 11, 2009).

9. Gereffi, G., and Dubay, K, Center On Globalization Governance & Competitiveness. (2008) Chapter 3: Auxiliary Power Units/ Reducing Carbon Emissions by Eliminating Idling in Heavy-Duty Trucks. http://www.cggc.duke.edu/environment/climatesolutions/greeneconomy_Ch3_AuxiliaryPowerUnits.pdf. (Accessed March 11, 2009).

10. Burtscher, H. and Majewski, W.A., "Particulate Matter Measurements," Ecopoint, Inc., 2004. www.dieselnet.com. (Accessed April 24, 2009).

11. Walsh, M. P., Bradow, R., "Diesel Particulate Control Around the World," SAE Technical Paper, 910130, 1991.

12. Heywood, J.B., *Internal Combustion Engine Fundamentals*, McGraw Hill, 1998.

13. Majewski, W.A., "Diesel Particulate Matter," Ecopoint, Inc., 2002. www.dieselnet.com. (Accessed April 24, 2009).

14. Trijonis, J.C. Impact of Light-Duty Diesels on Visibility in California. Journal of Air Pollution Control Association. 1982, 32 (10), 1048-1053

15. Lloyd, A.C., Cackette, T.A., Diesel Engines: Environmental Impact and Control. Journal of Air and Waste Management Association. 2001 51:809-847.

16. "Despite Lower Carbon Dioxide Emissions, Diesel Cars May Promote More Global Warming then Gasoline Cars," American Geophysical Union/Stanford University/National Science Foundation Joint Release, October 2002. http://www.agu.org/sci_soc/prrl/prrl0233.html. (Accessed January 21, 2009).

17. Jacobson, M.Z., "Control of fossil-fuel particulate black carbon and organic matter, possibly the most effective method of slowing global warming," Journal of Geophysical Research, vol. 107, October 2002.

18. Jacobson, M.Z., "Strong radiative heating due to the mixing state of black carbon in atmospheric aerosols," Nature, Vol. 409, January 2001.

19. Hansen, J. Nazarenko, L., "Soot climate forcing via snow and ice albedos," Proceedings of the National Academy of Sciences of the United States of America, vol. 101, January 2004

20. Schroder, J., Elsch-Paush, K., McLachlan, M.S. "Measurement of Atmospheric Deposition of Polycholrinated Dibenzo-p-Dioxins (PCDDs) and Dibenzofurans (PCDFs) to a Soil," Atmospheric Environment. 1997, 31 2983-2989.

21. Hostmann, M., McLachlan, M.S. "Atmospheric Deposition of Semivolatile Organic Compounds to Two Forest Canopies," Atmospheric Environment, 1998, 32 (10), 1799-1810.

22. Eisenreich, S.J., Simick, M.E., Panek, J.A., Swackhamer, D.L., Long, D.T., Golden, K.A., Liu, S.P., Lipiatou, E. "Atmospheric Loading of Polycyclic Aromatic Hydrocarbons to Lake Michigan as Recorded in the Sediments," Environmental Science and Technology. 1996. 30: 3039-3046.

23. Wik, M., Renburg, I., "Recent Atmospheric Deposition in Sweden of Carbonaceous Particles from Fossil-Fuel Combustion Surveyed Using Lake Sediments," Ambio. 1991. 20: 289-292.

24. Baedecker, P.A., Edney, E.O, Simpson, T.C., Hosker, R.P, McGee, E.S., "Effects of Acidic Deposition on Materials," State of Science and Technology #19. U.S. National Acid Precipitation Assessment Program: Washington, DC. 1991.

25. Baedecker, P.A., Reddy, M.M., Reimann, K.J., Sciammarella, C.A. "Effects of Acidic Deposition on the Erosion of Carbonate Stone – Results from the U.S. National Acid Precipitation Assessment Program (NAPAP)." Atmospheric Environment. 1992. B26. 147-158.

26. Zhang, X.Q., McMurry, P.H., Hering, S.V., Casuccio, G.S. "Mixing Characteristics and Water Content of Submicron Aerosol Measured in Los Angeles and at the Grand Canyon." Atmospheric Environment. 1993. 27A: 1593-1607.

27. Sawyer, R.F., Pitz, W.J. Assesment of the Impact of Light-Duty Diesel Vehicles on Soiling in California. A2-064-32. Prepared for the California Air Resources Board by Sawyer Associates. Berkeley, CA, 1983.

28. "Diesel Particulate Matter," Air Toxics in New England, EPA Website, updated May 2007, www.epa.gov/NE/eco/airtox/diesel.html. (Accessed January 5, 2009).

29. Walsh, M. P., Bradow, R., "Diesel Particulate Control Around the World," SAE Technical Paper, 910130, 1991.

30. "Diesel Exhaust: A Critical Analysis of Emissions, Exposure, and Health Effects," DieselNet Technical Report, Ecopoint, Inc., 1997. www.dieselnet.com (Accessed November 17, 2008).

31. Prisby, R.D., Muller-Delp, J., Delp, M.D., and Nurkiewicz, T.R., "Age, Gender, and Hormonal Status Modulate the Vascular Toxicity of the Diesel Exhaust Extract Phenanthraquinone," Journal of Toxicology and Environmental Health, Part A, 71, November 2007.

32. Bowman, C., "Diesel linked to truckers' deaths," Sacramento Bee article, January 2008. www.sacbee.com. (Accessed June 6, 2008).

33. California Air Resources Board Document: Health Effects of Diesel Exhaust Particulate Matter. Downloaded from CARB website. http://www.arb.ca.gov/research/diesel/dpm_health_fs.pdf (Accessed February 23, 2009).

34. US EPA (2002) Health Assessment Document for Diesel Engine Exhaust. National Center for Environmental Assessment, Office of Research and Development, U.S. Environmental Protection Agency, Washington, D.C.

35. "Verified Technologies," California Air Resources Board (CARB) website. www.arb.ca.gov. (Accessed January 20, 2009).

36. Ames, R. W., "Analysis of a 2007 EPA Compliant Diesel Particulate Matter Sampling System," M.S. Thesis, Department of Mechanical and Aerospace Engineering, West Virginia University. Morgantown, WV, 2007.

37. "Controlling Emissions From Diesel Engines" Dana Etherton of Mcklenburg County Air Quality: http://www.4cleanfuels.com/. (Accessed October 9, 2008).

38. Washington State University Extension Energy Program document. "Diesel Oxidation Catalyst" http://www.energy.wsu.edu/documents/renewables/DieselOxidation.pdf. (Accessed August 18, 2009).

39. Liu, Z.G., Berg, D.R., Schauer, J. J., "Detailed Effects of a Diesel Particulate Filter on the Reduction of Chemical Species, Emissions." SAE 2008-01-0333, 2008

40. Sandoval, J.A, Wayne, W.S., Posada, J., Schiavone, J., Pigman, E. "Emissions Reduction in Transit Buses: Westchester County's Proactive Approach" Submitted to the Journal of Transportation Research Forum, Spring 2008.

41. Diesel Particulate Filter Image, http://www.kr.cd-adapco.com/press_events/Dynamics/26/image/automotive/auto1.jpg. (Accessed February 20, 2009).

42. "What is a DPF – Disel Particulate Filter?" Online topic from About.com. http://alternativefuels.about.com/od/glossary/g/dpf/htm. (Accessed February 20, 2009).

43. S.Okada (Yanmar Co. Ltd.,), J.Senda, "Particulate Matter Emission in Steady State Operation and Transient Operation from Direct Injection (DI) Off-Road Diesel Engine", 7th Int. Conf. on Engines for Automobile (ICE2005), No.2005-24-017(2005-9), pp.1-8.

44. Montajir, R., Otsuki, Y., Inoue, K., Asano, I., Kihara, N., Horiba Ltd. Japan, "Solid and Volatile Particle Emission Behavior from a Small Non-Road Diesel Engine," SAE Technical Paper, 2007-32-0058, 2007.

45. US EPA Code of Federal Regulations Title 40, Part 1065. US Government Printing Office. http://ecfr.gpoaccess.gov. (Accessed June 6, 2009).

46. "Primary Head-Type Flowmeters for the Accurate Measurement and Control of Gases and Liquids," Venturi Flowmeter Bulletin 201. Flow-Dyne Engineering, Inc., Fort Worth, TX, 1999

47. Reschke, G.D. "Optimization of a Flame Ionization Detector for the Determination of Hydrocarbon in Diluted Automotive Exhausts." SAE 770141, 1977

48. Barnett, R. A., "Characterization of Infield Vehicle Activity Data and Exhaust Emissions from Diesel Powered Off-Road Vehicles," M.S. Thesis, Department of Mechanical and Aerospace Engineering, West Virginia University. Morgantown, WV, 2001.

49. ISO 8178 Diesel Emissions Test Cycle: http:/www.dieselnet.com/standards/cycles/iso8178.html. (Accessed August 4, 2009).

50. "Nonroad Diesel Engines: Emissions Standards," DieselNet website. http://www.dieselnet.com/standards/us/nonroad.php. (Accessed September 1, 2009).

51. Wayne, W. S., Dinex, Inc. DiSiC Aftertreatment System Verification for Transportation Refrigeration Units. West Virginia University, January 2009.

52. Nuszkowski, J., Thompson, G.J., Clark, N., "Experimental and Error Analysis Investigation into Dilution Factor Equations," SAE Technical Paper, 2007-01-0310. 2007

53. Doebelin, E.O., *Measurement Systems Application and Design*, McGraw Hill, 1990.

54. Clean Air Nonroad Diesel – Tier 4 Final Rule. EPA Website. http:///www.epa.gov/nonroad-diesel/2004fr.htm. (Accessed October 5, 2009).

55. US EPA Code of Federal Regulations Title 40, Part 1039. US Government Printing Office. http://ecfr.gpoaccess.gov. (Accessed September 7, 2009).

56. Final Regulation Order. California Code of Regulations, Title 13, Division 3. Chapter 14. "Verification Procedure, Warranty and In-Use Compliance Requirements for In-use Strategies to Control Emissions from Diesel Engines." http://www.arb.ca.gov/diesel/verdev/reg/procedure_jan1009.pdf. (Accessed October 6, 2009)

57. Nichols, M.D., California Air Resources Board Mail Out #MSC 08-26, "Deadline for installation of diesel emission control systems that do not comply with the 2009 Nitrogen Dioxide emission Limit," September 22, 2008. http://www.arb.ca.gov/diesel/verdev/mailout08262009.pdf. (Accessed October 6, 2009)

58. Hilliard, J.C., Wheeler, R.W., "Nitrogen Dioxide in Engine Exhaust," SAE Technical Paper 790691

59. DyneSystems, Inc. Website: DyneSystems, Inc. Midwest & Dynamatic Dynamometers. http://www.dynesystems.com. (Accessed February 25, 2009).

60. Lippert, T., P.F. Sherman Quotation #103239, Cincinnati Fan, "Dilution Tunnel Blower,"

# Appendix A: Additional Small Engine Test Cell Information

**Table A - 1: Test Cell Dynamometer Motor Specifications.**

| Description | | Specification Value | | |
|---|---|---|---|---|
| Model Number | | L1605A-V | | |
| Frame Type | | FL1844 | | |
| Rated Power | | 40 hp | | |
| Base Speed | | 3550 RPM | | |
| Phase/Hertz | | 3/120 | | |
| Volts | | 460 | | |
| Amps | | 53 | | |
| **Rated Full Load Data** | | | | |
| | **RPM** | **HP** | **Torque (ft-lbs)** | **Amps** |
| Base Speed | 3550 | 40 | 59 | 53.4 |
| Max Speed | 5323 | 40 | 39 | 47.9 |
| Min Speed | 0 | 0 | 59 | 53.4 |
| **Load Performance at Base Speed** | | | | |
| | **RPM** | **HP** | **Torque (ft-lbs)** | **Amps** |
| No Load | 3600 | 0 | 0 | 27.4 |
| 1/4 | 3588 | 10 | 15 | 30.6 |
| 1/2 | 3576 | 20 | 29 | 36.3 |
| 3/4 | 3564 | 30 | 44 | 44.1 |
| Full Load | 3500 | 40 | 59 | 53.4 |
| O/L | 3487 | 78.6 | 118 | 100 |

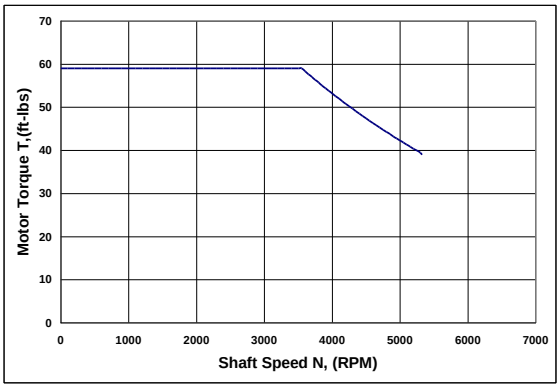


**Figure A 1: SETC Dynamometer torque curve.**

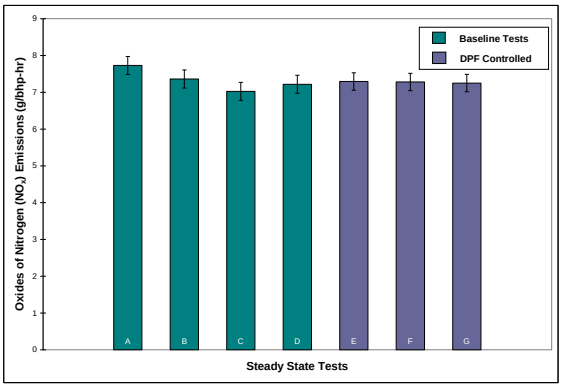


**Figure A 2: $NO_x$ emissions comparison for all tests.**

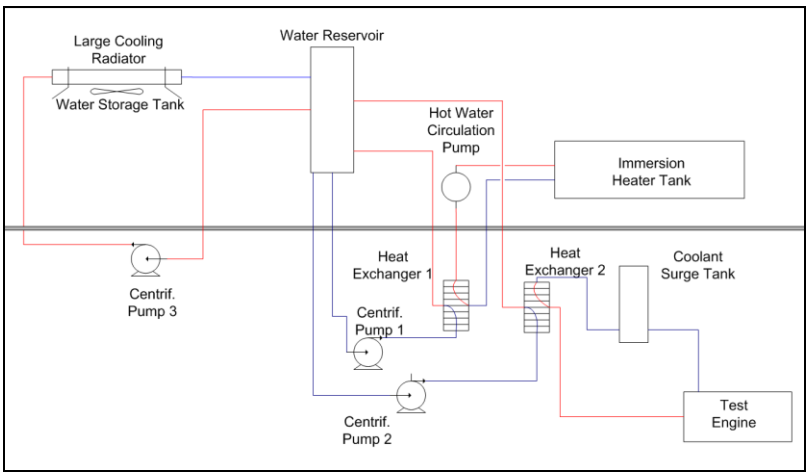


**Figure A 3: Test cell cooling system schematic.**

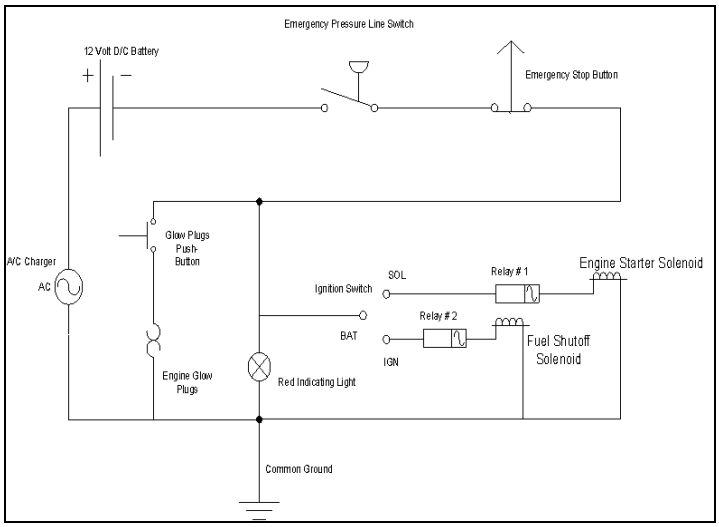


**Figure A 4: Engine ignition wiring diagram.**

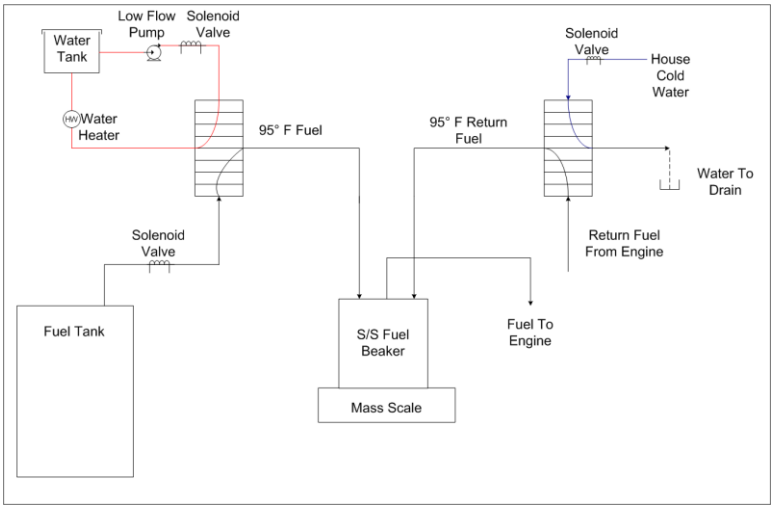


**Figure A 5: Fuel conditioning box schematic.**

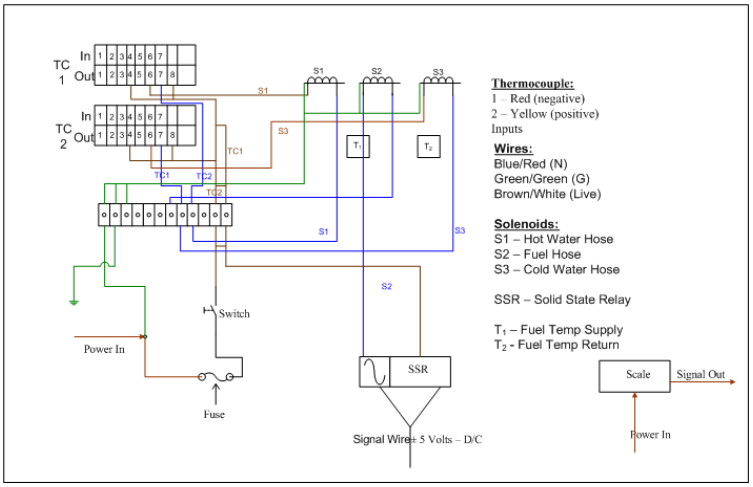


**Figure A 6: Fuel conditioning box wiring diagram.**

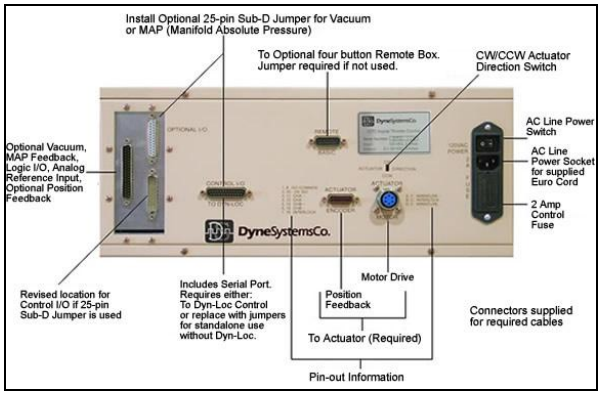


**Figure A 7: Rear panel of DyneSystems DTC-1 [59].**

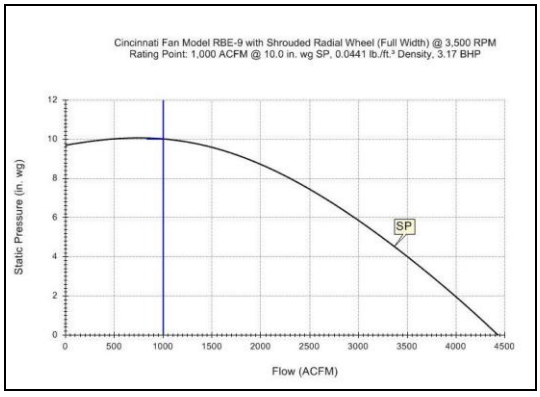


**Figure A 8: Performance curve for dilution tunnel blower [60].**